

# **Numerical Simulation of Benzene Transport in Shoreline Groundwater Affected by Tides**

Mahsa Kheirandish

A Thesis

in the Department of

Building, Civil and Environmental Engineering

Presented in Partial Fulfillment of the Requirements

for the Degree of

Master of civil engineering at

Concordia University

Montréal, Quebec, Canada

April 2021

© Mahsa Kheirandish, 2021

**CONCORDIA UNIVERSITY**  
**SCHOOL OF GRADUATE STUDIES**

This is to certify that the thesis prepared

By: *Mahsa Kheirandish*

Entitled: *Numerical Simulation of Benzene Transport in Shoreline Groundwater Affected by Tides*

and submitted in partial fulfillment of the requirements for the degree of

MASTER of SCIENCE (*Civil Engineering*)

Complies with the regulations of the University and meets the accepted standards with respect to originality and quality.

Signed by the final examining committee:

_____	Chair
<i>Dr. Fuzhan Nasiri</i>	
_____	Examiner
<i>Dr. Fuzhan Nasiri</i>	
_____	Examiner
<i>Dr. Biao. Li</i>	
_____	Supervisor
<i>Dr. Chunjiang An</i>	
_____	Supervisor
<i>Dr. Zhi Chen</i>	

Approved by \_\_\_\_\_  
*Dr. Michelle Nokken, Department Graduate Program Director*

\_\_\_\_\_ 2020 \_\_\_\_\_  
*Dr. Mourad Debbabi, Dean*  
*Gina Cody School of Engineering and Computer Science*

## **Abstract**

### **Numerical Simulation of Benzene Transport in Shoreline Groundwater Affected by Tides**

**Mahsa Kheirandish**

The release and transport of benzene in coastal aquifers were investigated in the present study. Numerical simulations were implemented using the SEAM3D coupled with GMS, to study the behavior of benzene in the subsurface of the tidally influenced beach. The transport and fate of the benzene plume were simulated, considering advection, dispersion, sorption, biodegradation, and dissolution in the beach. Different tide amplitudes, aquifer characteristics, and pollutant release locations were studied. It was found that the tide amplitude, hydraulic conductivity, and longitudinal dispersivity were the primary factors affecting the fate and transport of benzene. Aerobic biodegradation played a significant role in plume transport and benzene fate. The tidal amplitude could influence the travel speed and the percentage of biodegradation of benzene plume in the beach. A high tidal range reduced the spreading area and enhanced the rate of benzene biodegradation. Hydraulic conductivity had the impact on plume residence time and the percentage of contaminant biodegradation. Lower hydraulic conductivity induced longer residence time in each beach portion and a higher percentage of biodegradation in the beach. The plume dispersed and the concentration decreased due to high longitudinal dispersivity.

**Keywords:** numerical simulation; benzene; transport and fate; shoreline; groundwater; tide

## **Acknowledgments**

I would like to express my sincere gratitude to my supervisors, Dr. An and Dr. Chen, for their continuous support to my study and research, as well as their patience, motivation, and immense knowledge.

A special thanks to my family for supporting me spiritually throughout writing this thesis and my life in general. Words cannot express how grateful I am to my mother, Azar Danesh, father, Reza Kheirandish, brother Mahyar and sister Azadeh and my dearest brother-in-law Hamed for all the sacrifices that you've made on my behalf. Your prayer for me was what sustained me thus far. I would also like to thank all my friends who supported me in writing and incited me to strive towards my goal.

This research was also supported by the Multi-Partner Research Initiative of Fisheries and Oceans Canada and the Natural Sciences and Engineering Research Council of Canada.

# Table of contents

List of Tables .....	VII
List of figures.....	VIII
Chapter 1: Introduction.....	1
Chapter 2: Literature Review.....	3
2.1. Structure and Properties of Oil .....	3
2.2. Biodegradation of Petroleum Hydrocarbons .....	10
2.3. Numerical Models Ascertaining Petroleum Hydrocarbon Fate and Persistence.....	13
2.4. Summary of Literature Review.....	18
Chapter 3: Methodology .....	19
3.1. GMS Models.....	19
3.2. Numerical Implementation .....	20
Chapter 4: Results and Discussions .....	25
4.1. Model validation .....	25
4.2. Groundwater Flow Distribution.....	26
4.3. Fate and Transport of Contaminant .....	28
4.4. Effects of Tide .....	30
4.5. Effects of Hydraulic Conductivity.....	34
4.6. Effect of Longitudinal Dispersivity .....	40
Chapter 5: Conclusions.....	42

5.1. Conclusion .....	42
5.2. Research Contributions.....	43
5.3. Recommendations for Future Research.....	43
References.....	44

## List of Tables

Table 1: Significant chemical classes and structures of some example molecules.....	5
Table 2: Characteristics of the numerical experiments and different scenarios that are analyzed in this study.....	23
Table 3: Physical properties parameter values used in the numerical simulations.....	24
Table 4: Microbial parameters used in numerical model.....	24

## List of figures

Fig. 1: The most favorable temperatures of soil, freshwater, and marine environment for hydrocarbon degradation rates (Das & Chandran, 2011). .....	11
Fig. 2: a) The front view of the model grid. The leaking location is 110 m from the seaside and 50 m in the shoreline, and the groundwater table is 2 m below the surface. b) The schematic diagram of the three-dimensional model grid. c) The plan view of the leaking location on $x=50$ m with the contaminant concentration contours at $t=0$ . .....	21
Fig. 3: Evaluated aerobic biodegradation of benzene and simulation results using SEAM3D and models developed by other studies (Chen et al., 1992; El-Kadi, 2001; Essaid et al., 1995; Geng et al., 2017). The experimental results are reported in Chen et al. (1992). .....	26
Fig. 4: Velocity vectors and flow condition. a) Case 4 (no tide). b) Case 1 ( $A=1$ m). c) case 2 ( $A=2$ m). d) Case 3 ( $A=3$ m). .....	27
Fig. 5: Concentration contour in base scenario ( $A=1$ ) a) Fate and transport of the benzene after 7, 30 and 90 days. b) Oxygen consume due to microbial degradation after 7, 30 and 90 days. c) Nutrient concentration in domain after 7, 30 and 90 days .....	30
Fig. 6: Tide effect on the concentration of benzene in time at a different location: a) Tide effect on different scenarios (Case 1, 2, 3 and 4) at $x=60$ m (10 m after source point). b) Tide effect on case 1, 2, 4 at $x=130$ (80 m after the benzene release source). c) Benzene concentration at $x=130$ for case 3 (due to the small amount of benzene concentration in this location the graph has been shown separately). .....	32

Fig. 7: Spreading area of the benzene plume after 15 days affected by different tide amplitude in for the first scenarios, the area shrink due to an increase in the tide amplitude .....	33
Fig. 8: Checking the sensitivity of the model to a) hydraulic conductivity b) Specific yield c) Specific storage.....	35
Fig. 9: Effect of hydraulic conductivity on plume concentration during the specific time: a) concentration versus time at x=60 m (10 m after benzene released). b) and c) plume concentration versus time at x=130 (80 m after point source). .....	38
Fig. 10: Plume transport after 30 days. a) hydraulic conductivity 0.9 m/h (case 6). b) Hydraulic conductivity 1.8 m/h (case 1). c) Hydraulic conductivity 3.6 m/h (case 5).....	39
Fig. 11: Effect of longitudinal dispersivity on Benzene concentration during the time. a) Concentration of benzene 10 m after the point source. b) Concentration of benzene 80 m after releasing contaminant. ....	41

## Chapter 1: Introduction

Unexpected discharges of organic pollutants have been exerting an increasing effect on coastal aquifers in recent decades (Bi et al. 2020; Chen et al. 2019). Release from petrol stations, pipelines, and industrial activity, for instance, has a detrimental effect on shoreline groundwater (Boufadel et al. 2016; Dojka et al. 1998; Essaid 1994; Lee et al. 2015). In order to evaluate and remediate subsurface contamination, though, a deeper understanding of the status and transport mechanism of pollutants in groundwater is critical (Colombani et al. 2015; Liu et al. 2016). In coastal aquifers, due to the complex mechanisms underlying groundwater flow (e.g., tide, waves, dissolved solutes), identifying the residence time, fate, and natural degradation of the plume is a challenge (Geng et al. 2017).

Various studies have been carried out to investigate the behavior of groundwater and the plume transport in coastal aquifers (Santos et al. 2012). Several factors have been identified as affecting subsurface flow pathways and solute transport. For instance, tides can recirculate groundwater and seawater at the oceanic side of aquifers, making them a critical oceanic force (Heiss 2011; Li et al. 2008). Oil discharged to groundwater undergoes various processes that modify its structure and concentration. These chemical, physical, and biological processes have a significant impact on the toxicity and permanence of the pollution (Liu et al. 2012). Various physical remediation strategies have been applied in response to oil spills to eliminate or disperse the oil in order to mitigate its harmful effect on the environment. Microbial degradation, meanwhile, is a biological process that can be applied to clean up petroleum hydrocarbon contamination (Leahy et al. 1990). In the biodegradation process, petroleum hydrocarbons are typically electron donors. The electron acceptors vary from oxygen ( $O_2$ ) to sulfate ( $SO_4^{2-}$ ), nitrate ( $NO_3^-$ ), ferric ions (Fe (III)), oxidized manganese (Mn (IV)), and carbon dioxide ( $CO_2$ ). Microbes use the energy released from this redox reaction for microbial growth (Jorgensen et al. 1989).

A number of numerical models have been introduced by researchers based on particular field situations. Uraizee et al. (1997) constructed a mathematical model that considered the relationship

between the biodegradation of crude oil and the bioavailability parameter. A two-dimensional model was developed by Boufadel et al. (1999) to estimate the solute in relation to water density and viscosity using the MARUN model. Essaid et al. (2003) quantified BTEX dissolution and biodegradation of crude oil using the BIOMOC code combined with the UCODE. Li and Boufadel (2010) conducted two-dimensional variable density and saturation simulations using the MARUN model to assess the durability of the oil. Torlapati and Boufadel (2014) applied the numerical model, BIOB, to simulate the biodegradation of the oil captured in sediment. Xu et al. (2015) predicted the fate of spilled gasoline in soil and groundwater using the Hydrocarbon Spill Screening Model (HSSM) coupled with the modified Modular Three-Dimensional Multispecies Transport Model (MT3DMS). Although these works are encouraging, the knowledge about the fate and transport of petroleum pollutants in the shoreline groundwater is still limited. The impacts of some shoreline conditions such as tide are not clear.

Benzene is a natural component of crude oil, and it has been identified as a lethal chemical that can cause acute and chronic poisoning (Verma et al. 2002). Benzene is a low molecular weight aromatic that has a comparatively high solubility in water (Reddy et al. 2012). In this context, the objectives underlying the research presented in this paper are (a) to use the numerical model SEAM3D coupled with GMS as a reactive transport model to simulate transport and fate and complex biodegradation processes involving benzene and different electron acceptors (e.g., oxygen and nitrate); and (b) to identify the key factors influencing a pollution plume's fate in shorelines, such as tide amplitude and beach properties (i.e., hydraulic conductivity and longitudinal dispersivity).

## **Chapter 2: Literature Review**

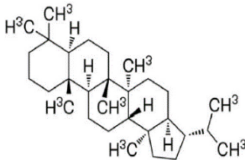
Each year, there is an average of 2,000 oil spills in the continental waters of the United States, although inland oil spills received significantly less attention than marine oil spills (Owens et al. 1993). While the number of freshwater spills is less than that in the marine environment, they pose significant potential risks to the environment due to the closeness to the water bodies with less dilution and dispersion capacity and include the shoreline directly impacted by the spill. Various habitats' shoreline ecosystems contain steep rock, movable pebbles, and clean sand of open shores to the soft mud. Various plant and animal species inhabit these ecosystems and provide food and awning to many others. Shorelines also deliver several advantages to nearby ecosystems and to the broader environment. The coastal aquifer can be affected by oil spills from shipping, marine investigation and production, pipelines, or land-based facilities. Oil contamination of shorelines impacts habitats and causes malfunctions in the services that they provide, which can affect the species' populations. Depending on the shoreline sediment's properties, the oil plume can infiltrate and reach the groundwater. Some of the factors that can affect the oil penetration include porosity, depth of groundwater table, oil properties such as viscosity.

### **2.1. Structure and Properties of Oil**

To grasp the oil spills' fate and transport in aquatic environments, an understanding of petroleum's chemical compound is essential. The chemistry of petroleum indicates its physical properties (e.g., density and viscosity), oil behaviour (e.g., dispersion, diffusion), and biological effects (e.g., toxicity, the capability to biodegrade). Various compounds of diverse sizes and classifications are present in crude oil, which consists of volatile compounds and nonvolatile compounds (Speight 2007) Hydrocarbon compounds are comprised of hydrogen and carbon, which are the main ingredients in oils. The chemical structure of crude oil changes due to the geological formation area and dramatically impacts the oil properties. A standard classification method is saturates,

aromatics, resins, and asphaltenes (SARA). The most abundant composites in oil or petroleum product are saturates, which are also the significant economic component of oils. They are called saturates because of the maximum number of hydrogens that they have. The saturate group of parts in oil comprises essentially of alkanes, and 50 to 90% of the crude oil typically consists of alkanes (Fingas et al. 2011). The aromatic compounds have a high stability ring due to the six equivalent carbons they have in the benzene ring. Therefore, benzene rings are remarkably persistent and can have toxic influences on the environment. Up to 60% of oil consists of polyaromatic hydrocarbons (PAHs) with at least two benzene rings. The resin's compound is mostly undiscovered, and they are the polar compounds that can be determined by precipitation or open column chromatography. Table 1 illustrates the significant chemical classes, including petroleum, and structures of some example molecules. The primary compounds that may exist in resins are nitrogen composites. Analyzing various resins indicates the existence of carbazole and alike components in these oils (Porter et al. 2004). Asphaltenes' structures and compounds are unknown, and they are represented by their sedimentation from oil in pentane, hexane, or heptane. The aromatic ring system is perceived to include about seven joined rings in the shape of a hand with the alkane chains expanding outer from the focal fused ring (Rodgers et al. 2007). Various microorganisms can biodegrade most of the alkanes under aerobic and anaerobic biodegradation trajectory while alkanes are chemically inert (Caldwell et al. 1998; Lee et al.1999; Rojo 2009).

**Table 1:** Significant chemical classes and structures of some example molecules.

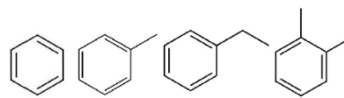
Chemical class	Example of class	Structure of example compounds	Characteristics
<b>SATURATES</b>			
n-Alkanes	<i>n-Hexadecane</i>		Most plentiful chemical class in petroleum; rarely water-soluble; biodegradable; commonly not toxic. Light liquids or gases are n-Alkanes with less than C6; toxic. The n-alkanes with C6-C18 are biodegraded easily. The ones with more than C20 are waxes and harder to biodegrade.
Hopanoids and Steroids	<i>17α(H),21β(H)-Hopane (30αβ)</i>		Most of them are hard to biodegrade; hence they are used as long-term biomarkers for biodegradation evaluation.

---

## AROMATICICS

The saturate class is frequently less toxic than this hydrocarbon class. When aliphatic groups are attached to the aromatic rings, many isomers and homologous series are possible.

Monoaromatics ***BTEX:***  
***Benzene,***  
***Toluene,***  
***Ethylbenzene***  
***and Xylene***  
***isomers (ortho-***  
***xylene shown)***



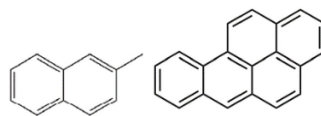
This series is volatile, and they have higher water solubility than other hydrocarbons. They are acutely toxic and/or carcinogenic and approximately biodegradable under aerobic and anaerobic conditions.

---

---

Polycyclic aromatic hydrocarbons (PAHs) and alkylated series (alkyl PAH)

2-  
*Methylnaphthalen*  
*e and*  
*Benzo[a]pyrene*



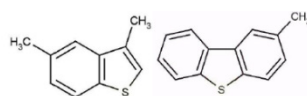
Due to multiple positions for alkyl side chains, many isomers are possible; Some of these compounds are toxic and/or carcinogenic. They are hardly biodegradable, so they have higher persistence in the environment. The US-EPA Priority Pollutant' is benzo[a]pyrene

This class has a lower molecular weight, lower aromatic content, and greater polarity than asphaltenes but with a solubility class related to asphaltenes.

## RESINS

Examples of S-containing moieties that may be constituents of resin molecules.

*Moieties may include:*  
*Dimethylbenzothio*  
*phene and 2-*  
*Methyldibenzo-*  
*thiophene*

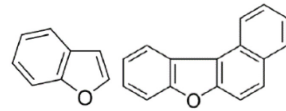


The total sulfur content of sour crude oils may contain these organic sulfur groups.

---

Examples of O-containing moieties that may be constituents of resin molecules.

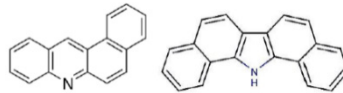
*Moieties may include: Benzo[*f*]naphthofuran;*



Photooxidation or partial biodegradation may generate the organic oxygen-containing groups in resins from PAHs.

Examples of N-containing moieties that may be constituents of resin molecules.

*Moieties may include: Benz[*a*]acridine; Dibenzo[*a,i*]carbazole*

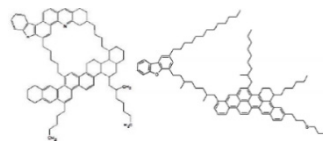


The polarity of the resins fraction presented by N-containing groups

## ASPHALTENES

A solubility class of complex high molecular weight (HMW), polar compounds that are not water-soluble; present to heavy oil viscosity; hardly biodegrade.

*Hypothetical asphaltene molecules, after Hoff and Dettman (2012) and Boek et al. (2010)*



The asphaltene models have numerous structures with various size, aromaticity, and degree of condensation.

---

The most common aromatic compounds found in the oil are Benzene, Toluene, Ethylbenzene, and Xylenes (BTEX). Due to the benzene ring's stability, aromatics are immanent and can have toxic influences on the environment. 0 to 2.5% of the oil structure comprises BTEX (Fingas et al. 2011). Experiments and simulations reveal that many BTEX compounds are very readily biodegraded by marine microorganisms. Previous studies reveal that BTEX compounds grow faster and have greater yield coefficients than multi-ring aromatics; therefore, they are better growth substrates (Chen et al. 1992; Atlas 1995; Godsy et al. 1999; Reardon et al. 2000). Polycyclic aromatic hydrocarbons (PAHs) contain more than two benzene rings and represent 0 to 40 percent of the oil composition (Fingas et al. 2011). The significant degradation process for PAHs is microbial degradation, although they may experience adsorption, volatilization, photolysis, and chemical degradation. PAH may be affected by adsorption, volatilization, photolysis, and chemical degradation; however, the significant degradation process for PAH is microbial degradation (both in aerobic and anaerobic conditions) ((Haritash et al. 2009); (Desai et al. 2008; Allan et al. 2012).

Due to various processes, the structure and concentration of the oil released into the oceans will change. Weathering, chemical, physical, and biological processes have a significant effect on the toxicity and persistence of the oil (Liu et al. 2012). The primary weathering processes are evaporation, dissolution, biodegradation, and photooxidation (Wang et al. 1999). The oil's extended vertical movement after the wellhead blowout and the dispersant could influence the weathering of crude oil. The composition of petroleum hydrocarbons in the oil collected from the ocean surface, oil deposited sediments, and salt marshes were examined in the field study (Liu et al. 2016). The information on petroleum hydrocarbon ascertains that the collected oil deposit from sediments was exposed to a light to moderate weathering degree, which was confirmed by the presence of short-chained n-alkanes, BTEX, and C3-benzene.

## 2.2. Biodegradation of Petroleum Hydrocarbons

Multiplex physical alternatives were used to eliminate or disperse the oil to resist the marine oil spill's disadvantageous environmental influence. Mechanical remediation, burying, evaporation, and washing are some of the regular methods to eliminate the hydrocarbons that contaminated the soil. These technologies are costly, and, in some cases, cause the incomplete breakdown of the contaminants. However, the petroleum hydrocarbon contamination's primary and final natural mechanism of clean up could be microbial degradation (Leahy et al. 1990; Atlas et al. 2011). The use of microorganisms to remove the pollutants or their toxicity due to a variety of microorganism's metabolic abilities is called bioremediation (Medina-Bellver et al. 2005). Microorganisms are available everywhere in marine environments to degrade oil (Prince 1993). Microbes that can degrade oil are ubiquitous, and various microbes that can degrade hydrocarbons will always situate in an aquatic environment. Microbes that can degrade oil will increase while the hydrocarbons are available, and they are more present in contaminated sites than in new sites. At the same time, overall microbial biodiversity reduces during the biodegradation processes, which relies on the physical and chemical properties of the compound and compound surface area. Petroleum hydrocarbon biodegradation is a complicated process that is contingent on aquifer characteristics and the amount of hydrocarbon existing (Atlas 1981). Some limiting agents influencing the biodegradation of petroleum hydrocarbons have been reviewed (Das et al. 2011). The availability of petroleum hydrocarbon to microorganisms is an essential factor limiting the biodegradation of oil in the environment. Hydrocarbon's capability to microbial degradation differs; linear alkanes have the most significant susceptibility, branched alkanes, small aromatics, and cyclic alkanes are ranked respectively (Ulrici 2000; Perry 1984). The petroleum hydrocarbon construction and inherent biodegradability component are the primary and initial essential factors that should be considered. Another vital physical agent that can affect both the chemistry of the pollutants and microbial activities is the temperature (Atlas 1975). The maximum degradation rate is in the range of 30–40°C in soil environments, 20°–30° in freshwater environments, and 15–20°C in marine environments (Bartha et al. 1984). Fig 1 indicates the ranging maximum degradation rate in different temperatures and environments. The amount of carbon remarkably rises due to significant oil spills in aquatic and freshwater environments; therefore, the nitrogen and phosphorus become a limiting agent for biodegradation. Prosperous petroleum hydrocarbons

biodegradation requires nutrients, especially nitrogen, phosphorus, and sometimes iron (Atlas 1985).

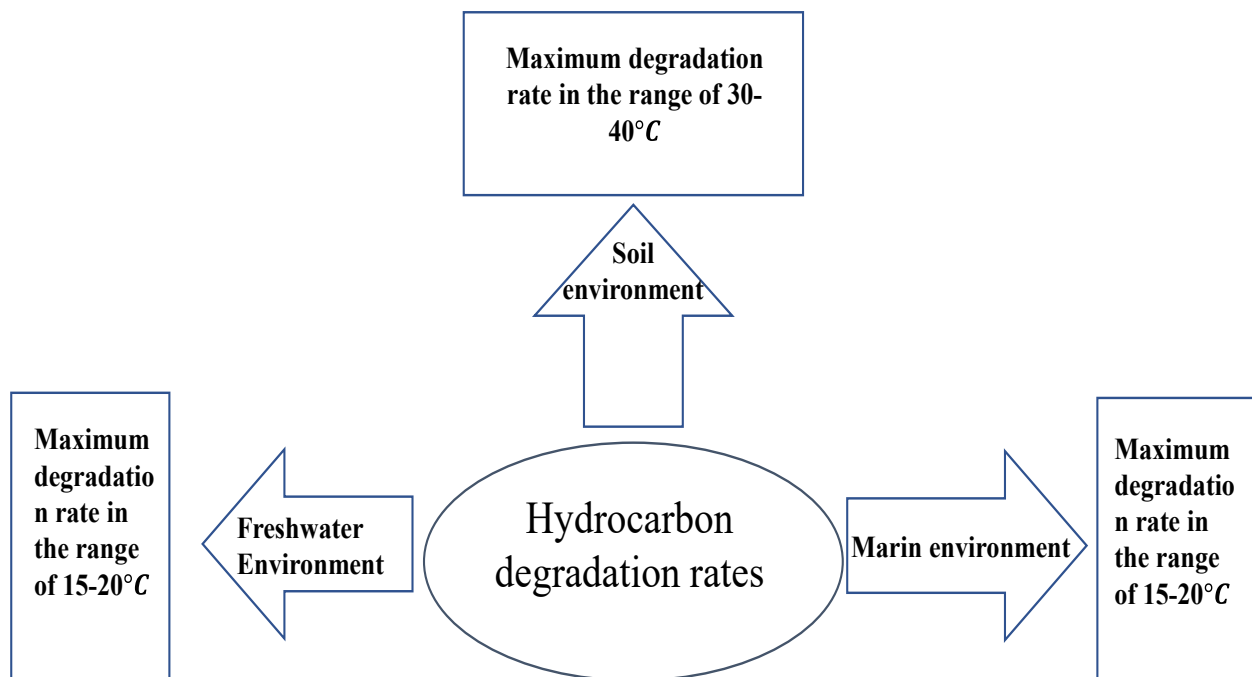


**Fig. 1:** The most favorable temperatures of soil, freshwater, and marine environment for hydrocarbon degradation rates (Das & Chandran, 2011).

The nature of petroleum hydrocarbon biodegradation is exchanging electrons; it is a redox chemical reaction that occurs between electron acceptors and electron donors. Microbes utilize the energy released from the redox reaction for microbial growth. In this redox reaction, the petroleum hydrocarbons are electron donors while electron acceptors vary from oxygen (O<sub>2</sub>), sulfate (SO<sub>4</sub><sup>2-</sup>), nitrate (NO<sub>3</sub><sup>-</sup>), ferric ions (Fe (III)), oxidized manganese (Mn (IV)), and carbon dioxide (CO<sub>2</sub>) (Jorgensen et al. 1989). The sequence of biodegradation processes depends on the availability of electron acceptors. The technical sequence of reactions is first aerobic degradation, then denitrification, followed by manganese and iron diminution, sulfate reduction, and methanogenesis (Lyngkilde et al. 1992; Vroblesky et al. 1994).

Although anaerobic biodegradation is considerable, aerobic biodegradation is more active. In aerobic conditions, organic pollutants degraded actively, faster, and completely. Since the

significant deterioration pathways for both saturates and aromatics initiate oxygenases, aerobic conditions are recognized as essential for the comprehensive degradation of oil hydrocarbons in the environment. In the primary stages of the biodegradation process, oxygen plays a cosubstrate role, and later it consumes as an electron acceptor for energy generation (Young et al. 1984). The significant agent that affected the biodegradation of Exxon Valdez oil in Alaskan beaches was low oxygen concentrations (Boufadel et al. 2010). Nitrogen-based compounds (nitrate, nitrite, and ammonia) are the restricting electron acceptors in most occurrences of aerobic biodegradation of hydrocarbon conditions in the oceanic environment (Venosa et al. 2010). The rate of oil biodegradation depends on the availability of inorganic nitrogen (N) and phosphorus (p) (Walker, 1984). The mass ratio of biomass uptakes is 10:1 of nitrogen/ phosphorus (Xia et al. 2006; Xia et al. 2005); therefore, significantly more nitrogen is needed for optimal microbial growth.

The biodegradation sequence relies on the availability of electron acceptors. Aerobic biodegradation is the accelerated degradation of the majority of the petroleum hydrocarbon. The class of oxygenases enzymes attacks the C-H bond in aerobic conditions while in anaerobic conditions, hydrocarbon degraders utilize alternate enzyme mechanisms (Boll et al. 2010). When oxygen is nonexistent, anaerobic biodegradation takes place and regularly presents less microbial growth rates compared with aerobic degradation. The anaerobic process has thermodynamic limitations of the terminal electron acceptor (TEA) and evaporation process; therefore, it has a lower microbial growth rate. Microbes tend to use the EAs that provide the highest Gibbs free energy when there are multiple EAs available (Waddill et al. 1998). The sequence that EAs utilize for microbial growth is  $O_2$ ,  $NO_3^-$ , Mn (IV), Fe (III),  $SO_4^{2-}$  and  $CO_2$  (Waddill et al. 2002).

The performance of spilled oil on sand and gravel coastline environments essentially depends on the characteristics of the soils, such as the substrate's porosity, the morphology of the coastline, and the energy of the tide or waves crashing the shoreline. The biomass and biological diversity, dissolved oxygen, and nutrient (N and p) replenishment will affect the fate of oil in marine and freshwater shorelines.

### **2.3. Numerical Models Ascertaining Petroleum Hydrocarbon Fate and Persistence**

The substrate and electron acceptor identified for the single-step biodegradation models' reaction, both electron donor and acceptor utilization, are managed kinetically (Schäfer et al. 1995). The biodegradation processes are divided into two half-cell reactions in the two-step biodegradation method. The first step is using the substrates and donates electrons, while the second step is reacting with electron acceptors to balance the donated electrons. Classical biodegradation transport is accompanied by complex bacterial growth inspired by single-step models, and the relations are based on Monod kinetics. The two-step process model assumed that the organic degradation step is rate-limiting, not the electron consumption step; this assumption relies on the Partial Equilibrium Approach (PEA). In simulating complex geochemical reactions, the two-step model reveals improvements; however, it has some drawbacks in simulating biomass growth (Jakobsen et al. 1999). Transportation and biogeochemical processes (both organic and inorganic reactions) can be simulated by mathematical models to estimate the long-term persistence of PHCs in the environment. Biodegradation models are distinguished regarding the comprehensive biodegradation process to a single-step process or a two-step process (Brun et al. 2002). A three-dimensional, two-step PEA model was developed by Brun and Engesgaard (2002) that provides Monod kinetics and biomass growth.

In the past, codes and software were generated based on numerical analysis to obtain a numerical solution to anticipate the fate and transport of oil in the environment. Corapcioglu and Baehr (1987) created a numerical model using the finite difference scheme to simulate the spilled oil trapped in the soil. They used the forwarding projection method to anticipate mass that enters the atmosphere or groundwater or was biodegraded and removed from the soil. Nicol et al. (1994) used the flooded column of porous media to develop a substructure for numerically modelling the biodegradation of petroleum. They categorized the petroleum hydrocarbon into eight ingredients and associated each degradable class with a specific microbial population. Monod kinetics were applied to model the biological processes and to determine the numerical equations. Moreover, a variable step, and variable order, backward differentiation method was used.

To evaluate and amend the contaminated subsurface area, a better comprehension of fate and transport of pollutants in groundwater has been indispensable (Brovelli et al. 2007; Colombani et

al. 2015; Liu et al. 2016; Lu et al. 1999; Sbarbati et al. 2015). In coastal aquifers, due to the complex groundwater flow mechanisms (e.g., tide, wave, dissolved solute), identifying the residence time, fate, and natural degradation of the plume is consistently a challenging issue (Geng et al. 2017). Therefore, many numerical models were created by researchers based on particular field conditions due to oil spill accidents. Various studies have been conducted to comprehend the groundwater behaviour and plume transport in coastal aquifers (Santos et al. 2012). Uraizee et al. (1997) developed a mathematical model based on the presumed bioavailability parameter to consider the relation of biodegradation of crude oil. The two-dimensional model was developed to evaluate the solute on water density and viscosity using the MARUN model by Boufadel et al. (1999). Cirpka et al. (1999) constructed the numerical models to estimate the impact of processing between substrates on microbial activity in the heterogeneous aquifer. Moreover, Essaid et al. (2003) quantified BTEX decomposition and biodegradation at a crude oil spill site placed near Bemidji, Minnesota, using the U.S. Geological Survey (USGS) solute transport and BIOMOC, the biodegradation code, coupled with the USGS universal inverse modelling code UCODE. The two-dimensional variable density and saturation simulations using a finite-element model MARUN estimate the long-term perseverance of oil from the Exxon Valdes spill carried out by Li and Boufadel (2010). Additionally, Vilcáez et al. (2013) applied a developing numerical model for the biodegradation of oil droplets to evaluate the time scale of the Deepwater Horizon (DWH) oil spill's fate in the Gulf of Mexico. Torlapati and Boufadel (2014) simulated the biodegradation of oil trapped in the sediment using the BIOB model.

Oil discharged to groundwater goes through various processes that modify the structure and concentration of the oil. These are known as chemical, physical, and biological processes, and have a vital impact on the toxicity and permanence of the pollution (Liu et al. 2012). Different physical alternatives were applied to eliminate or disperse the oil in order to mitigate the harmful effect of the oil spill on the environment. Due to microbial degradation as the primary and ultimate natural mechanism, petroleum hydrocarbon contamination could tidy up the polluted region (Colwell et al. 1977). In the biodegradation process, petroleum hydrocarbons are typically electron donors. The electron acceptors vary from oxygen (O<sub>2</sub>), sulphate (SO<sub>4</sub><sup>-</sup>), nitrate (NO<sub>3</sub><sup>-</sup>), ferric Ions (Fe(III)), oxidized manganese (Mn (IV)), and carbon dioxide (CO<sub>2</sub>). Microbes utilize the energy released from this redox reaction for microbial growth (Jorgensen et al. 1989). Borden and Bedient (1986) modeled the dissolved hydrocarbons biodegradation and assumed oxygen is

the only available electron acceptor. Due to an accidental oil spill, numerical models were formed by researchers based on particular field situations. Benzene is a natural component of crude oil, and it has been identified as a poisonous chemical able to cause acute and chronic poisoning (Verma et al. 2002). Essaid et al. (1995) constructed a model to simulate the biodegradation of volatile and non-volatile parts of dissolved organic carbon in both aerobic and anaerobic conditions. Clement (1999) considered various electron acceptors for the hydrocarbon biodegradation and transport of multispecies by developing a computer code called RT3D in a 3D groundwater system.

Some limited biodegradation models are considered the tide effect on fate and transport of hydrocarbon on shorelines El-Kadi (2001) constructed a hydrocarbon biodegradation model that reviews the kinetic utilization of oxygen and nitrogen. The model analyzed the flow in the saturated and unsaturated zone, species transport, heat transport, and bacterial growth processes. The outcomes illustrate that hydrocarbon biodegradation is significantly influenced by tidal action. The researcher did not explain the consequences of seawater intrusion and beach properties in their work. Hamed (2005) studied the transport of hydrocarbon contamination and predicted the plume persistence and level of a contaminant in the soil and groundwater. Moreover, Robinson et al. (2009) developed a numerical model study of the tidal action that affects the fate of BTEX released in an unconfined aquifer in a coastal beach. The simulations revealed that the time residency of the hydrocarbons increased due to tidal movements. The biodegradation rate increases in a tidal situation due to this long-time persistence compared with no-tide actions. The influence of nutrient limitations was not examined in this study. To simulate the biodegradation of the attached hydrocarbons that are not soluble, Geng et al. (2014) developed a numerical model called BIOB. The researchers used the empirical oil spill on Delaware Bay Beach (Venosa et al. 1996) to validate the model. They discovered that the biodegradation rate increased 3-4 folds when the nutrient concentration grew from 0.2 to 2.0 mg N/L.

Several factors have been recognized that affect subsurface flow pathways and solute transport. Tides can recirculate groundwater and seawater at the oceanic side of aquifers, making them one of the most critical oceanic forces (Boufadel 2000; Heiss, 2011; Li et al. 2008; Robinson et al. 2007). El-Bihery (2009) used MODFLOW to simulate the Quaternary groundwater system and discover the hydraulic parameters of the Quaternary aquifer to evaluate its recharge rate. They

applied SEAWAT to simulate the variable-density flow and seawater intrusion. In the Mediterranean basin, salinization caused by the extra utilization of these aquifers affects coastal aquifers. To study the singular and combined impacts of oceanic forces on the flow and mixing processes in a subterranean estuary shoreline, Xin et al. (2010) constructed a numerical model. The researchers found that increasing temperatures, rising sea levels, and decreasing the meteoric water precipitation due to global warming and climate change enhanced the salinization processes in Mediterranean coastal aquifers.

Bakhtyar et al. (2013) studied the transport of a changeable density and conservative contaminant in an unconfined shoreline aquifer affected by tides and waves. The results indicate that oceanic forcing creates an upper saline plume underneath the beach face as well as a classical saltwater split. Tides and waves impact the solute plume's transport path, persistence, discharge rate, and spreading area. Heiss and Michael (2014) constructed the numerical modeling and field study to examine the effects of tide stage on intertidal salinity and flow dynamics in sandy beach aquifers. Moreover, Steefel et al. (2015) reported the list of codes representing the flow, transport, and reactions in the subsurface environment. The models were PHREEQC, HPx, PHT3D, OpenGeoSys (OGS), HYTEC, ORCHESTRA, TOUGHREACT, eSTOMP, HYDROGEOCHEM, Crunch-Flow, MIN3P, and PFLOTRAN. The seasonal water table waving, tide magnitude, and tidal stage have a significant influence on the extent of the circulation cell and region of the mixing area. Xu et al. (2015) predicted the fate of spilled gasoline in soil and groundwater using the Hydrocarbon Spill Screening Model (HSSM) combined with the modified Modular Three-Dimensional Multispecies Transport Model (MT3DMS). The sensitivity analysis illustrates that both leakage rate and water saturation have an inverse relationship with the required time of gasoline through the vadose zone.

Li (2015) used the 3D sequential electron acceptor model (SEAM3D) to examine the geometry deposit of the potential effect of crude oil. The horizontal tar sheet and the spherical tarball were modeled, and the results demonstrate that the spherical deposits showed less blockage to groundwater flow compared to sheet geometry; therefore, this caused the greater sulphate reduction due to sulphate-based biodegradation of benzene. Essaid et al. (2015) studied the transport and fate of the NAPL in the subsurface by analyzing the simple systems with uniform characteristics toward complex system pore-scale and macro-scale heterogeneity. The researchers

also work on biodegradation of plume and multiple redox zone and microbial enzyme kinetics. Geng and Boufadel (2015) study the fate of solute in a laboratory beach and the effect of waves and tides on the fate of contaminant. The results show that waves enhance the exchange fluxes and produce a more expansive exchange flux zone along the beach surface. Waves caused plumes to go deeper and move more seaward in comparison with tide-only forcing. To simulate the low solubility hydrocarbon biodegradation and transport of contaminants in a tidally coastal environment. Geng et al. (2015) developed a numerical model, BIOMARUN, by coupling the Monod kinetic models, BIOB and MARUN. The key factors affecting the biodegradation of oil, such as permeability, capillary, and dispersivity, were examined by accomplishing sensitivity analyses in beaches.

Suk (2017) used the generalized integral-transform technique (GITT) and simulated the A one-dimensional, semi-analytical solution of solute transport. They studied the plume transport from a region in the tidally coastal aquifer as well as the plume shape and spatial plume moments. They also discovered that tide amplitude, hydraulic conductivity, and storage coefficient have a direct relationship with the macro dispersion coefficient while having an inverse relation with the storage coefficient. Geng et al. (2017) constructed the BIOMARUN model to investigate the fate and transport of hydrocarbon plume in both the saturated and unsaturated zones of a beach. They examined the tide amplitude, capillarity, and hydraulic conductivity as key factors that affect the biodegradation process. The results indicate that aerobic biodegradation plays a significant role in the fate of the contaminant and the centroid of plume influenced by tidal actions. Geng et al. (2017) investigated groundwater flow dynamics and moisture response to waves in the swash zone by combining field and numerical studies. In this study, they used the MARUN model and examined the hydraulic conductivity and capillary fringe property effect. The results show that increasing the hydraulic conductivity enhanced the swash-induced seawater infiltration into the beach. Simultaneously, a thicker capillary fringe reduced the available pore space for seawater penetration to the subsurface area.

Ghazal et al. (2018) applied the integrated model consisting of the SWAT, MODFLOW, and SEAWAT models to estimate Dissolved Silicate (DSi) fluxes' transport and fate on Hawaiian coastlines. They considered different scenarios such as wetland restoration, climate change, and sea-level rise. The results show that the climate change affected DSi fluxes in fresh submarine

groundwater discharge. In contrast, DSi fluxes did not change by wetland restoration. Gao (2018) applied GMS software to simulate groundwater pollution transport during a coastal polyurethane company's operation phase. They used MODFLOW to simulate the transport and groundwater flow and use MT3DMS to predict the contaminant plume's area and concentration. The outcomes illustrate that the migration distance and contaminant plume size extended with time, and the mass concentration of the plume decreased by increasing the diffusion distance. Geng et al. (2020) conducted a saturated groundwater flow model to study flow and solute transport in heterogenous tidally influenced beach aquifers. The outcomes reveal that heterogeneity significantly affects the spatial and temporal contaminant plume transport.

#### **2.4. Summary of Literature Review**

Numerous studies have explored the fate and transport of oil in the environment. Many studies created numerical models to simulate the spilled oil behaviour in the soil and groundwater aquifer based on particular field conditions. Several studies have been conducted to determine the groundwater behaviour and plume transport in coastal aquifers. Due to complex groundwater flow mechanisms, most of these studies identify the residence time, fate, and natural degradation of the plume based on the characteristics that affect oil transport and biodegradation. Most studies have been conducted on a two-dimensional numerical model. Some limited biodegradation models consider the tide effect on fate and transport of hydrocarbon.

## Chapter 3: Methodology

### 3.1. GMS Models

Environmental simulation is an important approach for investigating the pollutant transport and fate (Zhai et al. 2020; He et al. 2020; Asif et al. 2020). In the present study, numerical models are used to investigate and evaluate the validity of various studies available in the literature concerning (i) the situation and nature of flow-system boundaries, (ii) recharge and discharge locations, (iii) the hydrogeological framework. MODFLOW-2000 is a three-dimensional saturated groundwater flow model, and SEAM3D is a tool for modeling three-dimensional solute transport coupled with aerobic and sequential anaerobic biodegradation and dissolution of non-aqueous phase liquid (NAPL). In the present study, hydraulic heads and cell-by-cell fluxes are estimated using the MODFLOW model, while the flow simulation and SEAM3D are applied to model multiple solutes in a three-dimensional, anisotropic, heterogeneous aquifer subject to advection, dispersion, sorption, and biodegradation. These two models are implemented in a two-step (flow and transport) simulation following the groundwater modeling system (GMS).

MODFLOW, a finite-difference code coupled in the GMS, is applied in order to develop a steady- and unsteady-state groundwater flow model (Mehl et al. 2001). The three-dimensional flow of a subsurface of uniform density through porous ground, it should be noted, can be characterized using the following partial differential equation:

$$\frac{\partial}{\partial x} \left( K_x \frac{\partial h}{\partial x} \right) + \frac{\partial}{\partial y} \left( K_y \frac{\partial h}{\partial y} \right) + \frac{\partial}{\partial z} \left( K_z \frac{\partial h}{\partial z} \right) + W = S_s \frac{\partial h}{\partial t} \quad (1)$$

where  $K_x$ ,  $K_y$ , and  $K_z$  represent hydraulic conductivity along the  $x$ ,  $y$ , and  $z$  axes, respectively;  $h$  is the hydraulic head;  $W$  represents sources and sinks of water (the volumetric flux per unit of volume);  $S_s$  represents the specific storage;  $t$  is time. This equation is used to demonstrate the groundwater flow of the non-equilibrium state in heterogeneous and anisotropic soil. To achieve approximate solutions of this equation, numerical schemes such as the finite-difference method are applied based on the discretization of points in time and space (Anderson et al. 2015; Golchin et al. 2013).

The advection–dispersion equation is employed to describe the aqueous phase transport of all biodegradable substrates, electron acceptors, final products, mineral nutrients, and nonbiodegradable solutes. Equation 2 demonstrates the 3D transport of contaminants in groundwater:

$$-\frac{\partial}{\partial x_i}(v_i S_{ls}) + \frac{\partial}{\partial x_i} \left( D_{ij} \frac{\partial S_{ls}}{\partial x_j} \right) + \frac{q_s}{\theta} S_{ls}^* - R_{sink.ls}^{bio} + R_{source.ls}^{NAPL} = R_{ls} \frac{\partial S_{ls}}{\partial t} \quad (2)$$

where  $S_{ls}$  is the aqueous phase substrate concentration [ $M_{ls}L^{-3}$ ] for  $ls = 1, 2, \dots, NS$  (number of substrates);  $S_{ls}^*$  is the substrate point source concentration [ $M_{ls}L^{-3}$ ];  $v_i$  is the average pore water velocity [ $L T^{-1}$ ];  $x_i$  is the distance [ $L$ ];  $D_{ij}$  is the tensor for the hydrodynamic dispersion coefficient [ $L^2 T^{-1}$ ];  $R_{sink.ls}^{bio}$  is the substrate biodegradation sink term [ $M_{ls}L^{-3}T^{-1}$ ];  $R_{source.ls}^{NAPL}$  is the substrate source term due to NAPL dissolution [ $M_{ls}L^{-3}T^{-1}$ ];  $R_{ls}$  is the retardation factor for substrate  $ls$  [ $L^0$ ];  $t$  is time [ $T$ ];  $\theta$  is aquifer porosity [ $L^0$ ];  $q_s$  is the volumetric flux of water per unit volume of the aquifer [ $T^{-1}$ ] with  $q_s > 0$  for sources and  $q_s < 0$  for sinks. In the case of a point sink, the concentration is generally not specified, and the model uses  $S_{ls}^* = S_{ls}$  (Widdowson et al. 1988). The model follows Monod kinetics for biodegradation of each substrate. The effects of electron acceptors and nutrient availability, inhibition, and threshold concentration are also considered in the Monod equations.

### 3.2. Numerical Implementation

The domain of the flow and transport model has a length of 200 m with a slope of 4% (i.e., 200 cells) in the  $x$ -direction (domain length), 10 m (i.e., 10 cells) in the  $y$ -direction (domain width), and 25 m (i.e., 3 layers) in the  $z$ -direction (domain depth) as shown in Fig. 2. In the present study, the top elevation for the bottom layer is 10 m, while the middle layer has a 5 m thickness, and the top elevation of this layer is 15 m. The top elevation of the surface layer, meanwhile, is 25 m on the shoreline side, and, due to the slope, about 19 m on the seaside. However, the upper layer's hydraulic head changes with time (different tide levels), resulting in transient seaside boundary conditions governed by the tides. The inland head is about 23 m (2 m below the beach surface)

and the seaside head is about 19 m in the no-tide state while it ranges from 22 to 24 m under different tide conditions. The cosine function is approximated for the tide at the seaside, as follows:

$$H_{tide} = H_0 + A \cos\omega t \quad (3)$$

where  $H_0$  is the average sea level ( $H = 21$  m);  $A$  is the tide amplitude ( $A = 1, 2,$  or  $3$  m);  $\omega$  is the tidal angular frequency ( $\omega = 0.26$  rad/hr);  $t$  is the tidal period. The density difference between coastal water and groundwater is an essential component for most aquifer systems, while there are various scenarios that density effects are negligible. For example, based on different tracers like an isotopic compound of Cl and Sr, the deep saline water exists for some shoreline groundwater (Khaska et al. 2013). In the present study, the density effect is not significant for mixing simulation.

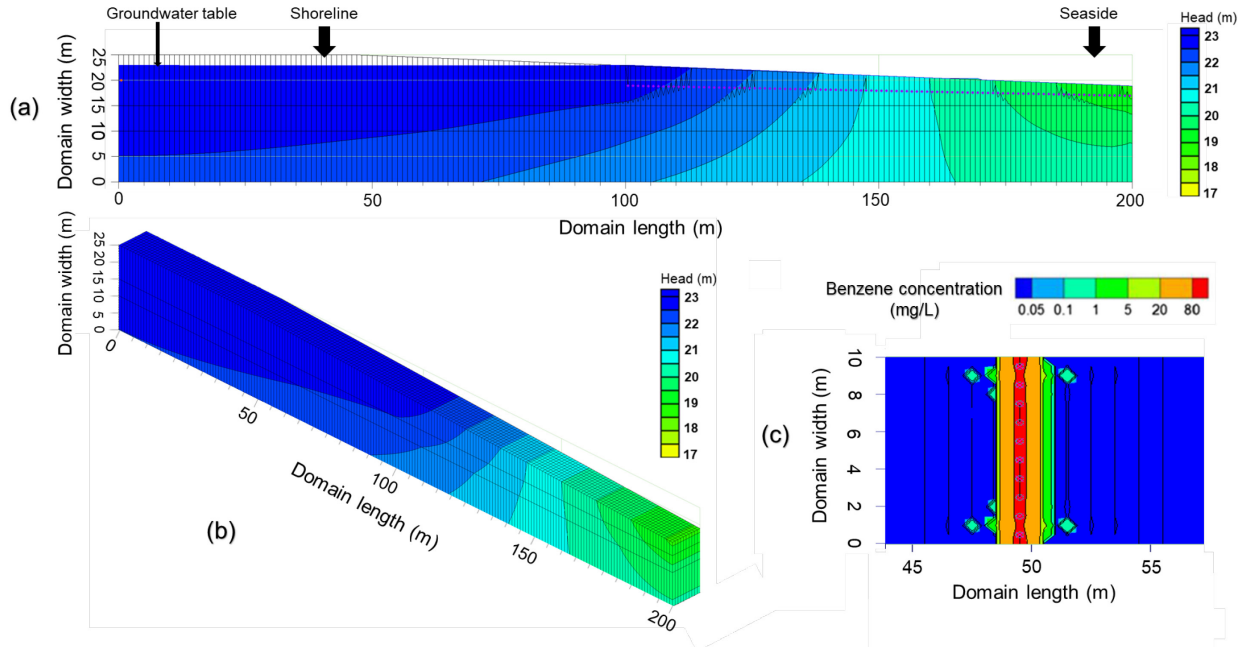


**Fig. 2:** a) The front view of the model grid. The leaking location is 110 m from the seaside and 50 m in the shoreline, and the groundwater table is 2 m below the surface. b) The schematic diagram of the three-dimensional model grid. c) The plan view of the leaking location on  $x=50$  m with the contaminant concentration contours at  $t=0$ .

The domain characteristics (e.g., hydraulic conductivity and longitudinal dispersivity) and the boundary inputs to the model to simulate the transport and fate of the benzene, nutrients, and oxygen are obtained from (Geng et al. 2015) for a tidally affected seashore in the Gulf of Mexico. The concentration of nitrate is found to be 1.2 mg-N/L in the shoreline and 0.2 mg-N/L at the seaside. The overall oxygen concentration in the whole area under consideration is 8.2 mg/L. It is assumed that the benzene has been released into the shoreline accidentally through the point source ( $1 \times 10 \text{ m}^2$  landfill) positioned at  $x = 50 \text{ m}$ , which is 110 m away from the seaside. The contaminant release period is 15 days at a benzene concentration of 100 mg/L (Geng et al. 2017). The parameters of microbial kinetics applied in simulating the biodegradation of benzene are obtained from Chen et al. (1992), Essaid et al. (1995), and El-Kadi (2001). The values of these parameters are assumed to be uniform in all layers of the aquifer in the three-dimensional model. The concentrations of aerobes and nitrate reducers at the outset of the simulation are consistent throughout the aquifer. The starting biomass of aerobes is higher than that of the nitrate reducers, given the theory that aerobic biomass will predominate when the domain has a significant oxygen level under primary conditions. The aerobic biomass of  $5 \text{ g/m}^3$  corresponded to  $16.6 \times 10^6 \text{ cells/cm}^3$ , assuming a cell volume of  $1 \text{ } \mu\text{m}^3$ , cell density of  $1.0 \text{ g/cm}^3$ . Therefore, the high amount of aerobic maximum utilization rate and the quantity of the cell's permissive considerable aerobic uptake of hydrocarbon substrates to occur instantly. However, anaerobic microbes can only survive in anaerobic microenvironments if they are inside soil aggregates (Brock et al. 2003). Hence, the nitrate reducer concentrations are a magnitude lower than the aerobic biomass concentrations.

The yield coefficients are applied in the model to determine the theoretical microbe growth resulting from the degradation of hydrocarbon substrates. As per the calculations reported by Bailey and Ollis (1986), the stoichiometric coefficient for oxygen utilization based on complete mineralization is set to 3.47 mg of  $\text{O}_2$ /mg of substrate. The yield coefficient for oxygen and nitrogen consumption during the complete mineralization of biomass is 1.56 mg of  $\text{O}_2$ /mg of microcolonies and 0.15 mg of N/mg of microcolonies, respectively (Bailey et al. 1986). For the simulations, the model, MODFLOW, is run for the unsteady condition flow. The SEAM3D model, meanwhile, is used for the fate and biodegradation of hydrocarbon. The stress period to simulate the flow and transport and biodegradation on the beach is 6 months.

Eight scenarios are simulated to investigate the effect of tide amplitude and beach properties (i.e., longitudinal dispersivity, hydraulic conductivity). The parameter values of each scenario are shown in Table 2, where scenario 1 is considered the base case. The properties of aquifer considered are summarized in Table 3. Table 4 shows the microbial parameters used in numerical model.

**Table 2:** Characteristics of the numerical experiments and different scenarios that are analyzed in this study.

<b>Scenario</b>	<b>Tide Amplitude (m)</b>	<b>Longitudinal Dispersivity (m)</b>	<b>Hydraulic Conductivity (m/h)</b>
<b>1</b>	1	0.3	1.8
<b>2</b>	2	0.3	1.8
<b>3</b>	3	0.3	1.8
<b>4</b>	0	0.3	1.8
<b>5</b>	1	0.3	3.6
<b>6</b>	1	0.3	0.9
<b>7</b>	1	0.6	1.8
<b>8</b>	1	0.1	1.8

**Table 3:** Physical properties parameter values used in the numerical simulations

<b>Definition</b>	<b>Unit</b>	<b>Value</b>
<b>Porosity</b>	/	0.3
<b>Hydraulic Conductivity</b>	m/h	1.8
<b>Specific Storage</b>	1/m	$10^{-4}$
<b>Vertical anisotropy</b>	/	10
<b>Horizontal anisotropy</b>	/	1
<b>Longitudinal Dispersivity</b>	<i>m</i>	0.3

**Table 4:** Microbial parameters used in numerical model

<b>Microbial properties</b>	<b>Units</b>	<b>Value</b>	<b>References</b>
<b>Distribution coefficient of benzene</b>	$m^3/g$	$3.6 \times 10^{-8}$	Essaid et al. 1995
<b>Initial mass fraction of benzene</b>	/	0.05	Geng et al. 2015
<b>Solubility of benzene</b>	mg/L	1780	Essaid et al. 1995
<b>Inhibition coefficient of <math>NO_3-O_2</math></b>	$g/m^3$	0.6	Waddill et al. 2002
<b>Stoichiometric coefficient for oxygen consumption based on complete mineralization</b>	mg of $O_2$ /mg of S	3.47	Geng et al. 2015
<b>Stoichiometric coefficient for oxygen consumption during the complete mineralization of biomass</b>	mg of $O_2$ /mg of X	1.56	Geng et al. 2015
<b>Stoichiometric coefficient for nitrogen consumption during the complete mineralization of biomass</b>	mg of N/mg of X	0.15	Geng et al. 2015
<b>Dissolved rate</b>	1/day	0.05	Gang et al. 2017

## Chapter 4: Results and Discussions

### 4.1. Model validation

The experimental data reported by Chen et al. (1992) is run in the SEAM3D model for validation as well as for the purpose of predicting the aerobic biodegradation and transport of benzene. Chen et al. (1992), it should be noted, presented both experimental and simulation results for benzene transport and biodegradation in a water-saturated soil column with a continuous flow. In their study, fixed amounts of benzene (20 mg/L) and hydrogen peroxide (132.7 mg/L O) are released to the column and benzene concentration samples are analyzed accordingly in the simulation. The porosity and longitudinal dispersivity are found to be 0.38 and 0.0224 m, respectively. The kinetic parameter values are obtained from (Essaid et al. 1995) who determined these values based on laboratory measurements and literature review. These data have been used to validate various reactive solute transport models in past studies (Essaid et al. 1995; El-Kadi 2001).

Fig. 3 shows the experimental data, as well as the results achieved by the SEAM3D and those obtained by the models in other studies (Chen et al. 1992; Essaid et al. 1995; El-Kadi 2001; Geng et al. 2017). It can be seen that the modeling with BIOMOC overpredicts benzene concentration. Chen et al. (1992) reported that the estimate of benzene degrader biomass underpredicted benzene concentrations. Therefore, the models and experimental data's difference remains within the range of uncertainty in the model parameter evaluation. SEAM3D is able to delineate the subsurface transport of various solutes in a 3D, anisotropic, heterogeneous region subject to advection, dispersion, adsorption, and biodegradation. This model can be used to simulate complicated biodegradation problems such as multiple substrates and multiple electron acceptors. As shown in the figure, the SEAM3D model is proven effective in representing the aerobic biodegradation and transport of benzene in the soil column.

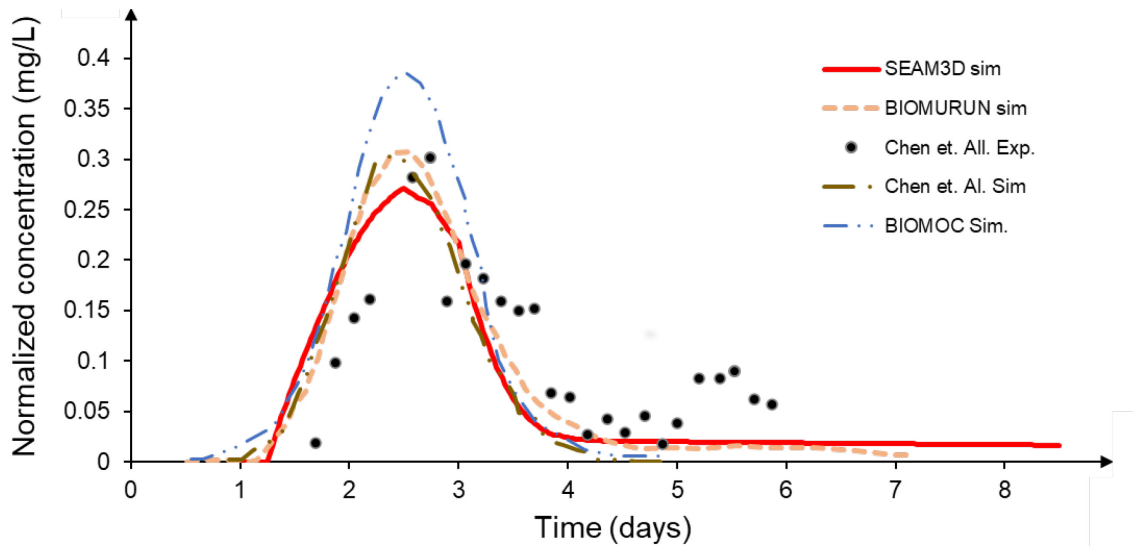


**Fig. 3:** Evaluated aerobic biodegradation of benzene and simulation results using SEAM3D and models developed by other studies (Chen et al., 1992; El-Kadi, 2001; Essaid et al., 1995; Geng et al., 2017). The experimental results are reported in Chen et al. (1992)

#### 4.2. Groundwater Flow Distribution

In this study, groundwater flows vertically downward through the three-dimensional model grid. In the base scenario, the tide amplitude is 1 m and the upper hydraulic head changes with time in a range of 19 to 22 m. In other scenarios, the tide amplitude changes to 2 and 3 m, with the maximum hydraulic head of 23 and 24 m, respectively. The hydraulic head of the upper boundary on the seaside changes with time in different scenarios due to the tide effect, thus, resulting in transient groundwater flow in terms of magnitude and flow direction.

Fig. 4 shows the groundwater flow and velocity fields in response to different tide levels when the tide is under the highest condition. In particular, Fig. 4a shows the model contours and the velocity magnitude of transient flow in the no-tide state; as can be seen, terrestrial groundwater flow discharges from the beach to the sea near the intersection between the shoreline and mean sea level. The flow transports from the shoreline (with higher groundwater level on the left side) toward the seaside and discharges to the sea. Fig. 4b illustrates the flow condition with the tide amplitude of

1 m and the tide exposure about 30 m toward the beach. As the tide amplitude increases, the span of the intertidal zone increases, as shown in Fig. 4c and Fig. 4d, the tide exposure for tide amplitudes of 2 and 3 m are 60 and 90m, respectively. At high tide condition, the groundwater table is elevated toward the shoreline side. Due to the tide effect, the front water affects the groundwater flow. Increasing the tide amplitude causes an increase in the intertidal zone and intrusion of the seawater to groundwater, having the impact on the groundwater flow velocity and direction. The downward movement occurs with increasing tides, while the seaward flow occurs mainly as tides fall (Bhosale et al. 2002).

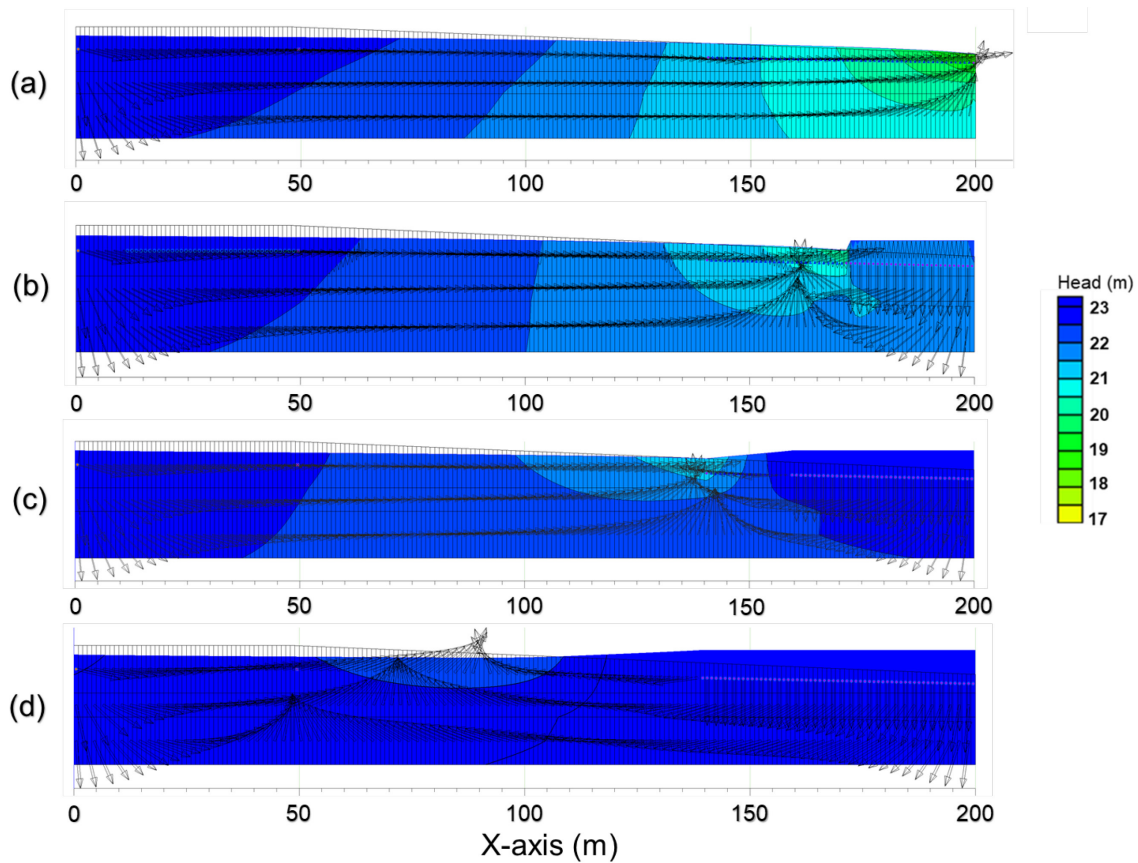


**Fig. 4:** Velocity vectors and flow condition. a) Case 4 (no tide). b) Case 1 (A=1 m). c) case 2 (A=2 m). d) Case 3 (A=3 m).

### 4.3. Fate and Transport of Contaminant

Fig. 5 shows the transport of the benzene plume and dissolved oxygen and nutrient concentrations in the beach after 7, 30, and 90 days of the primary contaminant discharge. Due to the constant release in the first 15 days, the benzene plume extends around its source point, as shown in the figure. It is evident that the plume of contaminant is expanding in the seaward and downward directions due to the fact that the regional groundwater hydraulic gradient is in a seaward direction. Movement deeper into the beach facilitates transport of the plume in the groundwater, as well as causing greater expansion in the downward direction. After 15 days, the benzene release ceases and the contaminant plume begins to relocate and move seaward. As can be seen in the figure, the benzene plume concentration begins to diminish at this juncture since it has left its source point. This could be the result of dispersion in the surrounding groundwater and biodegradation.

The simulation shows that approximately 99% of benzene is biodegraded on the beach before being released to the sea. Low oxygen and nutrient plumes are produced on the beach following the benzene's initial release due to biodegradation and associated microbial degradation. The oxygen reduction plume initially expands around the source point of the contaminant and moves seaward, with the behavior that is in line with the expected evolution of a benzene plume. The reduction of the oxygen and nutrient plumes, meanwhile, is due to the hydrocarbon biodegradation. Following the primary benzene discharge, bacteria degrade the benzene and convert it to biomass, carbon dioxide, and water. However, for aerobic biodegradation, the dissolved oxygen is required as an electron acceptor and nutrients are needed for growth and for functions such as ATP production. In fact, 3 g of oxygen is needed in order for 1 g of carbon to biodegrade. Therefore, the amount of oxygen required for biodegradation is greater than the number of nutrients required. Fig. 5 illustrates that the low oxygen plume formed is considerably larger than the size of the nutrient consumption plume in the shoreline. Moreover, the model results show that natural degradation is a critical process as the contaminant plume migrates. Simultaneously, the dissolved oxygen conditions are a vital indicator for evaluating the fate of benzene.

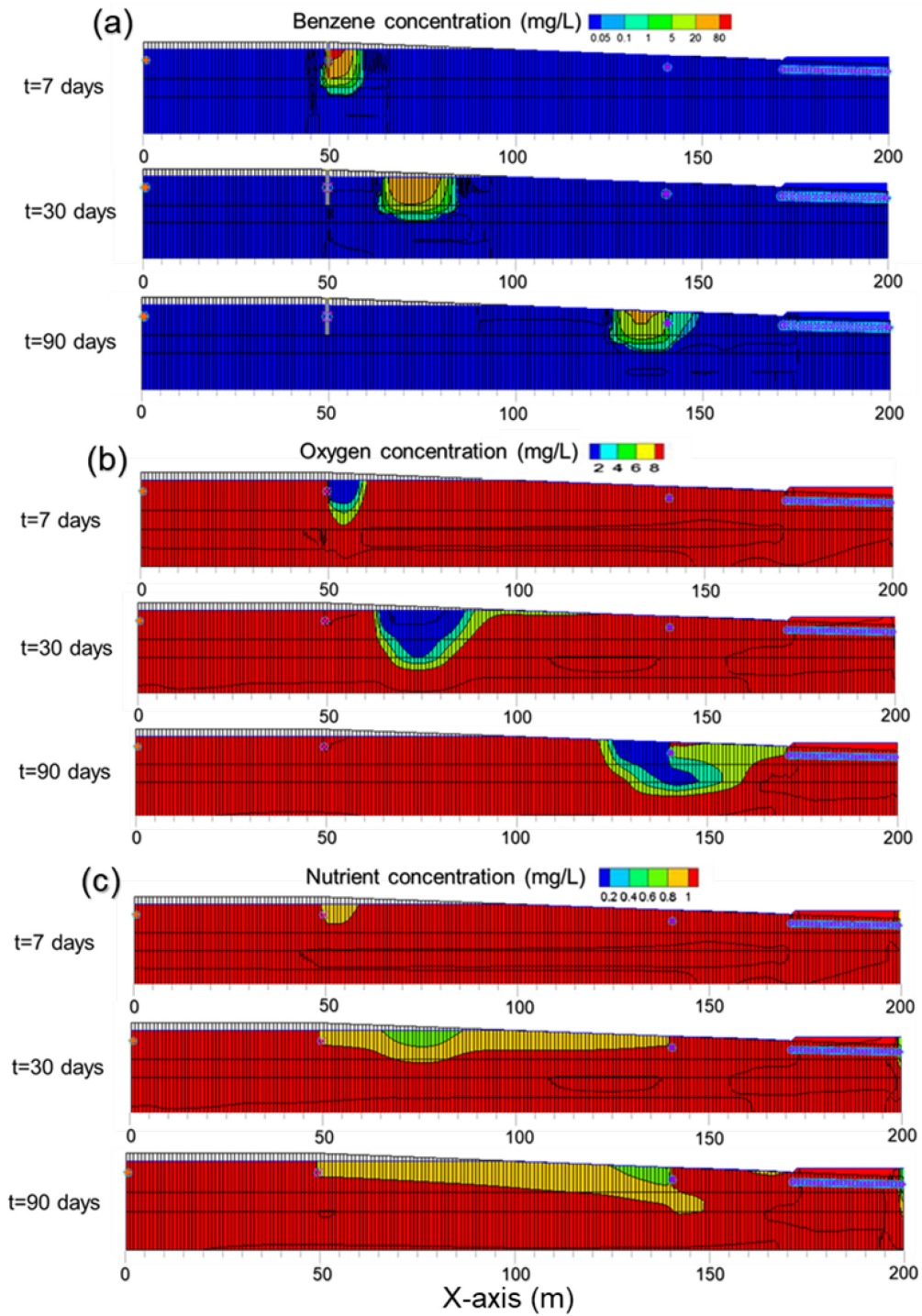


**Fig. 5:** Concentration contour in base scenario ( $A=1$ ) a) Fate and transport of the benzene after 7, 30 and 90 days. b) Oxygen consume due to microbial degradation after 7, 30 and 90 days. c) Nutrient concentration in domain after 7, 30 and 90 days

#### 4.4. Effects of Tide

The environmental conditions may often play an important role in the pollutant transport and fate (Ordieres-Meré et al., 2020; Shrestha et al. 2020). In the present study, four simulations are conducted with different tidal amplitudes ( $A = 1, 2, 3,$  and  $0$  m) in order to investigate the effect of tide on the fate and transport of contaminants in the beach. As shown in Table 2, case 1 ( $A = 1$ ) is considered the base case with which the other cases are compared. Fig. 6 reports the concentration of benzene (mg/L) in relation to time (day) in different locations. As mentioned above, the point source location is at  $x = 50$  m. Fig. 6a illustrates the concentration of benzene after 40 days at  $x = 60$  m (10 m after the release position), while Fig. 6b and Fig. 6c represent the concentration of benzene at  $x = 130$  m (80 m downwards from the benzene point source location in the saturated zone).

Fig. 6a shows that the plume reaches this location ( $x = 60$  m) in cases 1, 2, and 4 with the tide amplitude of 1 m, 2 m, and no tide, whereas in case 3 (tide amplitude = 3 m) the benzene plume transports 10 m from the point source location with a lag of approximately two days. The figure shows that the benzene concentration is affected by the tide amplitude, as well. For instance, the concentration of benzene in case 3 ( $A = 3$ ) is almost 10 mg/L less than that in the base case, signaling greater plume dispersion and chemical reaction than in the base case. The maximum concentration transport of benzene in cases 2 and 3, meanwhile, is almost the same as in case 1. As shown in Fig. 4, the tidal zone is different in each case; in cases 1 and 2, the tidal zone is 120 and 110 m, respectively, from the point source release, while, in case 3, the tidal zone is 90 m from the source, meaning that the effect of tide amplitude in case 3 is more significant.

Fig. 6b and Fig. 6c represent the benzene concentration in relation to time at the point 80 m far from the benzene release and 70 m from the seaside. It can be seen that, in case 1 ( $A = 1$  m), 22%

of the benzene reaches this location, while this proportion is 15% for case 2 ( $A = 2$  m), 0.00033% for case 3 ( $A=3$ ), and 25% for case 4 (no tide). It is also found that approximately 99% of the benzene is biodegraded on the beach before being released to the sea. The results show that 30% of the benzene released is biodegraded within 10 m of the release point, and almost 70% within 80 m. Fig. 6c shows that the tide tends to augment the dispersion and chemical reaction effects on the plume; accordingly, the amount of benzene that reaches point  $x = 130$  is very small compared to other situations. A high tide amplitude serves to enhance the seawater infiltration phenomenon in the shoreline and increase the groundwater table near the beach's seaward location. Since the tidal zone starts at 140 m in case 3, the effect of the tide is significant, and it has a circulating graph due to the sinusoidal tide function.

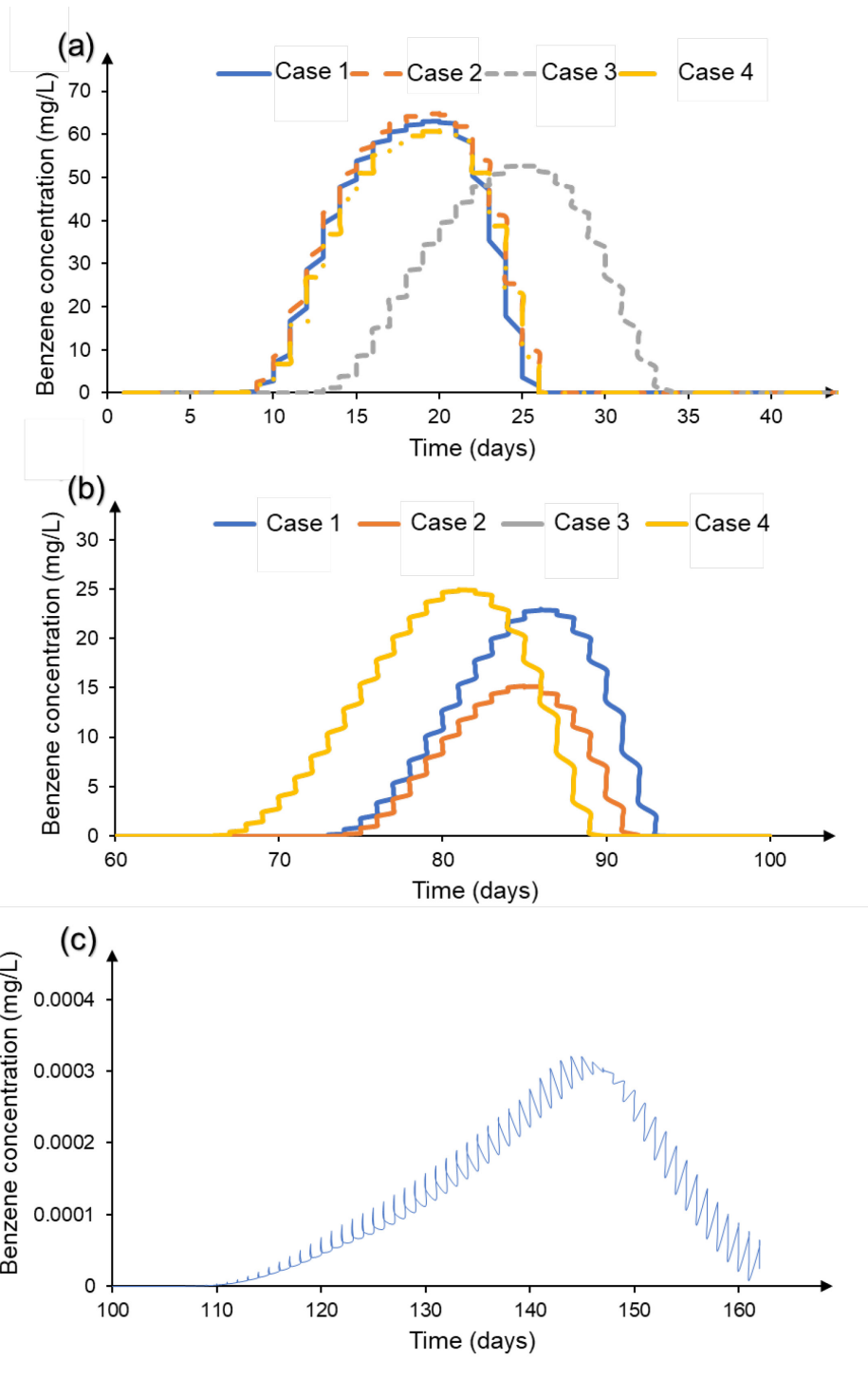


**Fig. 6:** Tide effect on the concentration of benzene in time at a different location: a) Tide effect on different scenarios (Case 1, 2, 3 and 4) at  $x=60$  m (10 m after source point). b) Tide effect on case 1, 2, 4 at  $x=130$  (80 m after the benzene release source). c) Benzene concentration at  $x=130$  for case 3 (due to the small amount of benzene concentration in this location the graph has been shown separately).

Fig. 7 shows the spreading area of the plume after releasing benzene under different tide amplitude conditions. As the tide amplitude increases, the spreading area shrinks, and this effect is more pronounced in case 3 due to the high tide amplitude and the zone affected by the tide. In cases 1, 2, and 4, the benzene plume spreads approximately 180 to 200 m while, in case 3, the benzene plume extends just 110 m. It is shown that when the tide amplitude increases, the span of the intertidal zone increases. With 1-m tide amplitude, the tide exposure is about 30 m toward the beach, while the distances are 60 and 90 m for tide amplitude of to 2 and 3 m, respectively. At high-tide conditions, the groundwater table is elevated toward the shoreline side.

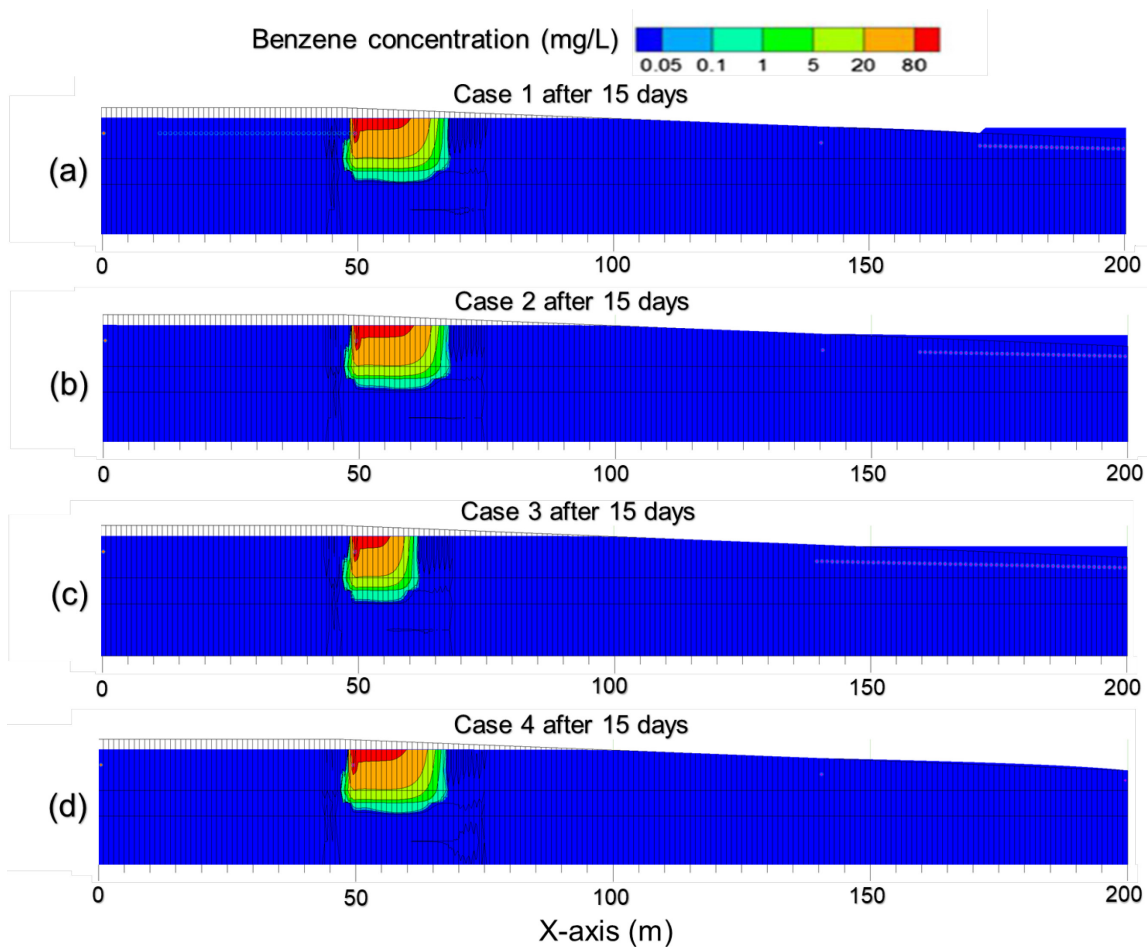


**Fig. 7:** Spreading area of the benzene plume after 15 days affected by different tide amplitude in for the first scenarios, the area shrink due to an increase in the tide amplitude

#### **4.5. Effects of Hydraulic Conductivity**

Different scenarios are simulated to investigate the effect of various beach characteristics on plume transport and fate. Various soil properties, such as hydraulic conductivity, specific storage, and specific yield, affect plume transport. The sensitivity analysis shows that the simulation model is most sensitive to hydraulic conductivity changes among these properties. Fig. 8 represents the sensitivity of the model to hydraulic conductivity, specific storage, and specific yield. This figure illustrates changing the hydraulic conductivity has a significant effect on the numerical model while varying specific storage and specific yield doesn't have a remarkable impact on the simulation model.

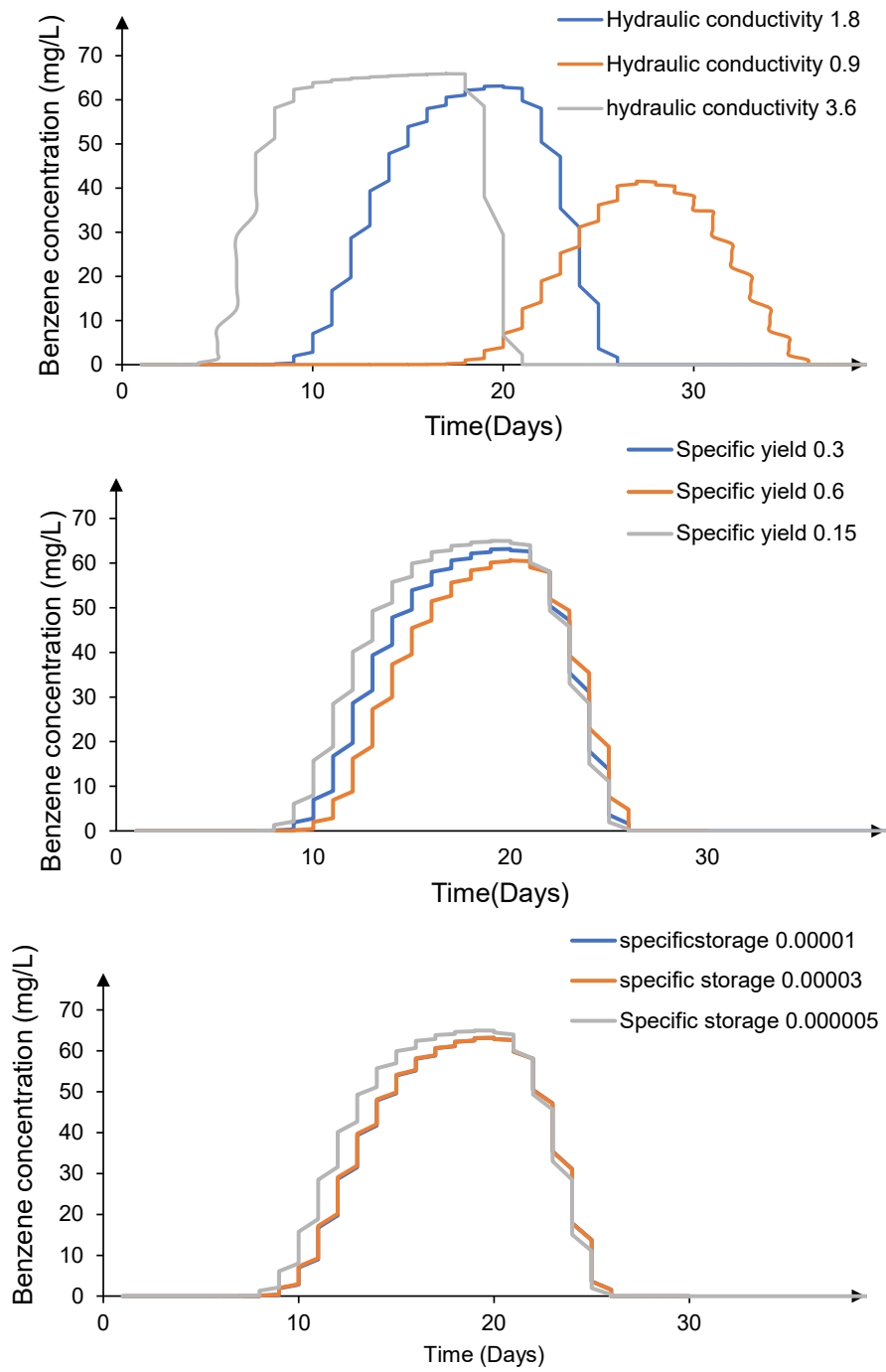


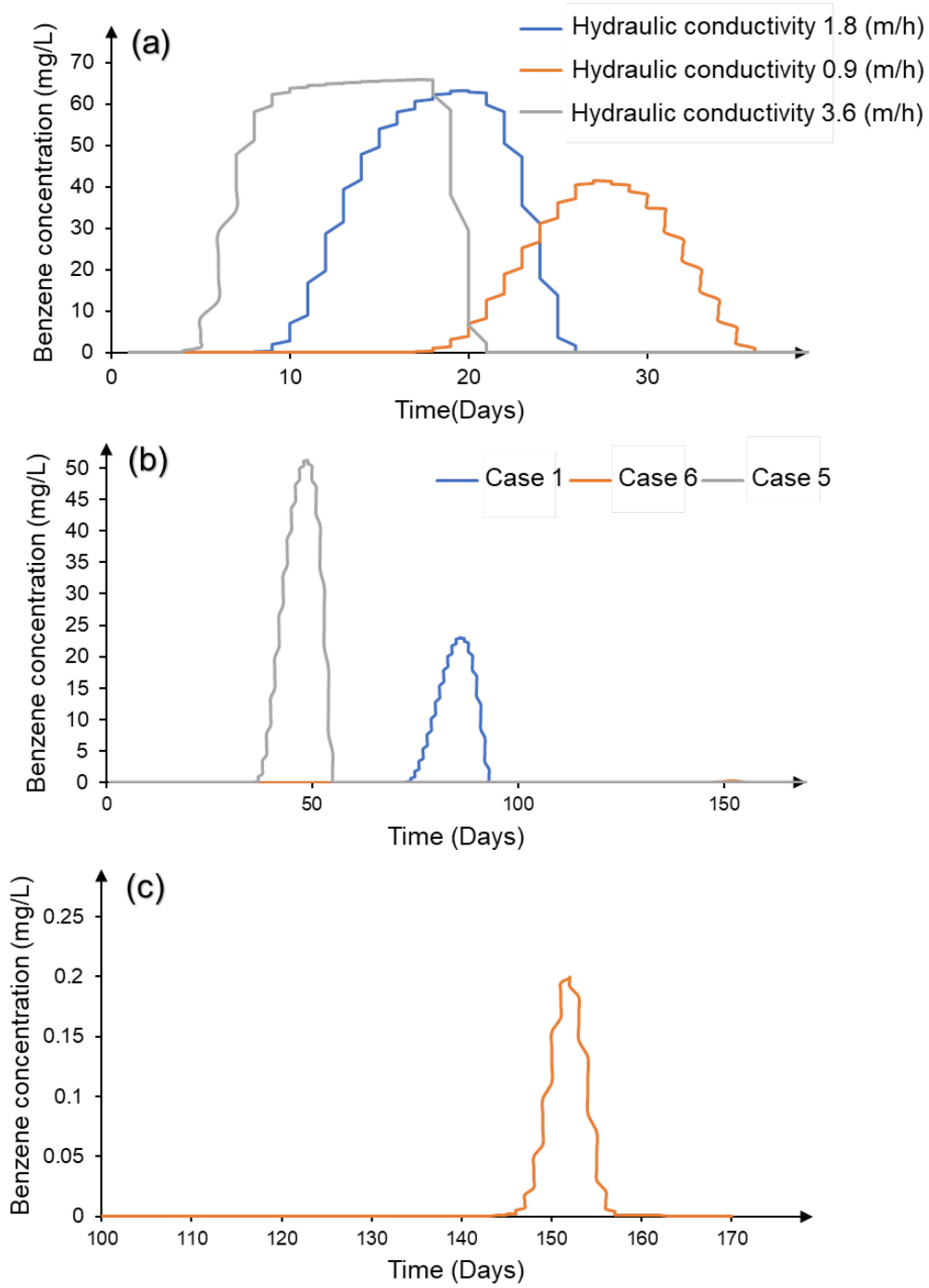
**Fig. 8:** Checking the sensitivity of the model to a) hydraulic conductivity b) Specific yield c) Specific storage.

Different scenarios are simulated to investigate the effect of various beach characteristics on plume transport and fate. Various properties, such as hydraulic conductivity, specific storage, and specific yield, affect plume transport. The sensitivity analysis shows that the simulation model is most sensitive to hydraulic conductivity changes among these properties. As such, in this section, hydraulic conductivity changes and the corresponding effect on benzene transport are discussed. Hydraulic conductivity, it should be noted, describes the ability of the soil to transfer fluid through voids. The hydraulic conductivity range for the coastal aquifer can be from 0.049 to 8.09 m/h (Lathashri et al. 2016). As Table 2 shows, cases 5 and 6 have different hydraulic conductivities (3.6 and 0.9 m/h, respectively). To better understand the effect of hydraulic conductivity, these two cases are compared to case 1 (1.8 m/h) as shown in Fig. 9. Fig. 9a represents the effect of different hydraulic conductivities on the amount of benzene transport 10 m after point source and the associated time lag for plume transport.

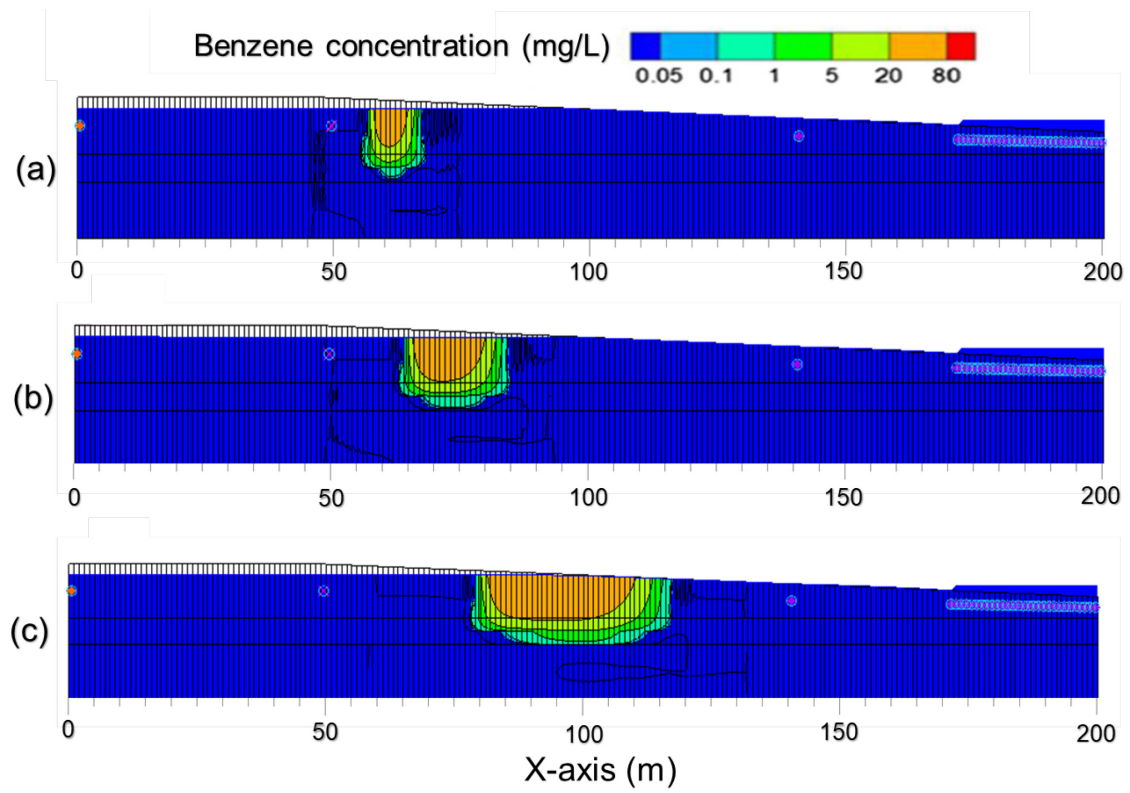
The results show that, in the base case (case 1), 60% of the benzene reaches the point,  $x = 60$  m, after 20 days. In comparison, the maximum concentrations transferred to this point in cases 5 and 6 are 66 mg/L (after 17 days) and 41 mg/L (after 27 days), respectively. Fig. 9b and Fig. 9c shows the benzene concentration that reaches the saturated zone ( $x = 130$  m) after a specific time in different situations. In case 1, approximately 80% of the benzene is biodegraded before reaching this point. In contrast, this proportion is 50% for case 5 and 99% for case 6. The diagrams also show that, in the beach with more permeable soil, the plume transport is faster, and as such the benzene's microbial degradation is lower. Due to the low hydraulic conductivity in this case, the plume moves slower, meaning that the contaminant's residence time at the beach is longer and the plume has a longer resistance to degrade at each part of the beach. In case 6, due to the longer residence time at  $x = 60$  m zone and adequate oxygen replenishment, a greater promotion of the contaminant is biodegraded along its pathways compared to in case 5. The significant goal for successful bioremediation is to maximize the oil's residence time in the beach and subsequently contacting microorganisms (Boufadel et al. 2006).

Fig. 10 demonstrates that hydraulic conductivity affects the plume expansion significantly. As shown in Fig. 10a with respect to case 6, the plume expansion is minimal after 30 days and it is still in the unsaturated zone. As shown in Fig. 10c with respect to case 5, in contrast, the plume

expansion is greater and it reaches the saturated zone. These results indicate that hydraulic conductivity is an important consideration when assessing the resistance of pollution in coastal beaches. The simulation results also demonstrate that hydraulic conductivity can affect considerably the plume degradation rate at various parts of the shoreline.



**Fig. 9:** Effect of hydraulic conductivity on plume concentration during the specific time: a) concentration versus time at  $x=60$  m (10 m after benzene released). b) and c) plume concentration versus time at  $x=130$  (80 m after point source).



**Fig. 10:** Plume transport after 30 days. a) hydraulic conductivity 0.9 m/h (case 6). b) Hydraulic conductivity 1.8 m/h (case 1). c) Hydraulic conductivity 3.6 m/h (case 5).

#### 4.6. Effect of Longitudinal Dispersivity

Longitudinal dispersivity is one of the main beach properties that may affect the plume transport and fate. Therefore, in this research, two cases are considered in order to observe the consequences of longitudinal dispersivity changes. Fluid does not move at uniform velocity throughout the soil; instead, mixing occurs along flow paths in a phenomenon known as longitudinal dispersion. Longitudinal dispersivity values obtained from experiments and simulations range from 0.07 to 11 m for different kind of sandy aquifers (Schulze-Makuch 2005). As shown in Table 2, cases 7 and 8 have different longitudinal dispersivities—0.6 m, and 0.1 m, respectively—compared to case 1 (0.3 m). Fig. 11a shows the simulation results of cases 1, 7, and 8 at point  $x = 60$  m (10 m after benzene release), while Fig. 11b shows the results when the plume passes 80 m into the beach (i.e.,  $x = 130$  m). The results show that the maximum plume concentration is reached at point  $x = 60$  m in approximately 20 days in all cases.

Fig. 11a indicates about 63% of the benzene released in the groundwater reaches  $x = 60$  m in case 1, while this proportion is 59.5% for case 7 and 64% for case 8. The results for different longitudinal dispersivity cases 80 m after point source are shown in Fig. 11b. As can be seen, by the time the longitudinal dispersivity doubles, 88% of the benzene has dispersed and biodegraded along its flow path. In comparison, this proportion is about 77% in the base case and 60% when the longitudinal dispersivity is 0.1 m. The simulation results illustrate that changing the longitudinal dispersivity does not significantly affect the plume duration transport, while it does affect considerably the concentration of benzene. In other words, the plume disperses and biodegrades during its transport, causing a reduction in the contaminant concentration. Therefore, when the longitudinal dispersivity increases, so too does the dispersion, and the benzene concentration decreases accordingly.

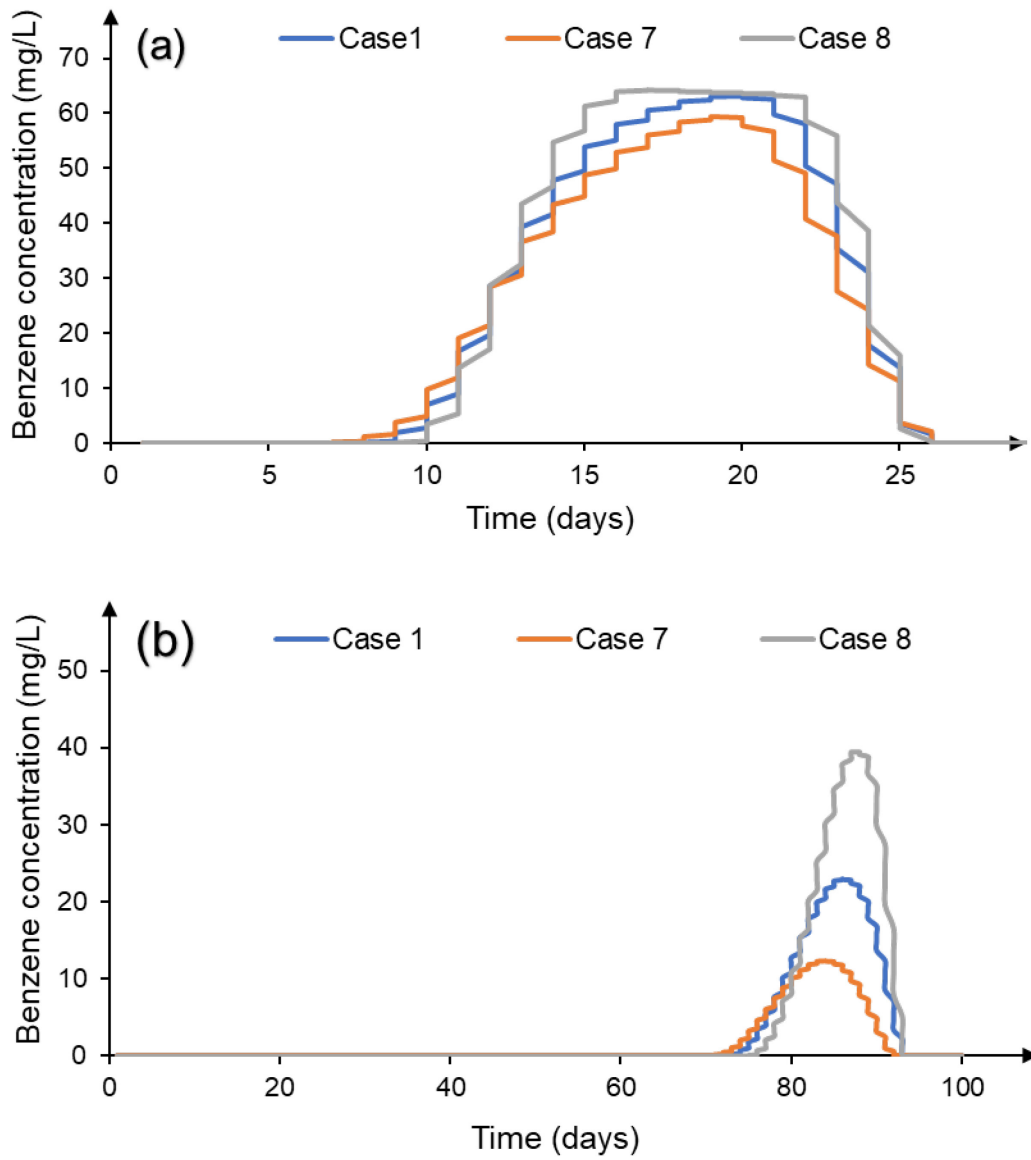


**Fig. 11:** Effect of longitudinal dispersivity on Benzene concentration during the time. a) Concentration of benzene 10 m after the point source. b) Concentration of benzene 80 m after releasing contaminant.

## Chapter 5: Conclusions

### 5.1. Conclusion

The research presents the use of numerical model, SEAM3D, to study the transport and biodegradation of benzene released into shoreline tide-affected groundwater. The simulation outcomes indicate the following. First, in tide-influenced beaches, aerobic biodegradation plays a significant role in plume transport and benzene fate, particularly when the point source is far from the sea zone. In microbial biodegradation, a large amount of oxygen is required, so a low-oxygen plume emerges in the groundwater. Second, benzene released to the groundwater is found to biodegrade up to 70% in beach aquifers, meaning that 30% of the initial benzene release is discharged into the ocean. Third, an increase in tide amplitude serves to augment the microbial biodegradation due to the significant increase in the plume's residence time. Moreover, a higher tide amplitude makes the contaminant plume smaller and reduces the spreading area of the pollution. Fourth, hydraulic conductivity has an enormous impact on the biodegradation rate in beach groundwater. For instance, when the hydraulic conductivity decreases from 3.6 m/h to 0.9 m/h, the benzene biodegradation percentage at  $x = 60$  m increases from 34% to 59%. Finally, longitudinal dispersivity also affects the concentration of benzene passing through its flow path to the sea without biodegrading. Increasing this property from 0.1 to 0.6 m, the percentage of biodegraded and dissolved benzene in the saturated zone increases from 60% to 88%. In this paper, it should be noted, our focus is on tidally-influenced aquifer systems of either freshwater or saltwater (but not a combination of both), and therefore density effects and associated freshwater–saltwater mixing is not considered. Density gradients generated by mixing between terrestrial fresh groundwater and seawater have been found to have a significant effect on nearshore flow and transport processes (Boufadel 2000; Geng et al. 2020). Although the density difference between seawater and terrestrial freshwater is an important consideration in most aquifer systems, there are numerous scenarios in which the density effects are negligible. For example, studies have found that saltwater can intrude as far as 15 km inland in some coastal aquifers, e.g., near the Persian

Gulf (Ataie-Ashtiani et al. 2013) . In addition, pore water salinity in tidal freshwater marshes can be as low as 3%, and therefore density gradients are negligible in these tidally-influenced aquifer systems (Baldwin et al. 2001; Mitsch et al. 2009). The findings of the present study are applicable to such scenarios.

## **5.2. Research Contributions**

In this study, the fate and transport of benzene on the shoreline groundwater have been investigated. The main contributions are as follows.

- Aerobic biodegradation plays a significant role in the fate of benzene on the tidally influenced beaches.
- Tide amplitude has a remarkable impact on microbial biodegradation due to the long persistence time of the contaminant plume.
- Hydraulic conductivity is a soil property that has a crucial effect on contaminant plume transport and fate.
- Longitudinal dispersivity is another soil property that affect the benzene's fate and transport, and its effect has been investigated in this research.

## **5.3. Recommendations for Future Research**

This study investigated benzene's transport and fate in a homogenous beach aquifer affected by tide using the SEAM3D software. Future studies be further conducted in the following areas.

- Develop a model with a heterogeneous beach aquifer subjected to the tide.
- Investigate the effect of density on the coastal beach subjected to the tide.
- Study the effect of the oil release conditions on the fate and transport of the oil in groundwater.

## References

- Allan SE, Smith BW, Anderson KA (2012) Impact of the Deepwater Horizon oil spill on bioavailable polycyclic aromatic hydrocarbons in Gulf of Mexico coastal waters. *Environmental science & technology* 46(4): 2033-2039.
- Anderson MP, Woessner WW, Hunt RJ (2015) *Applied groundwater modeling: simulation of flow and advective transport*: Academic press.
- Asif Z, Chen Z (2020) A life cycle based air quality modeling and decision support system (LCAQMS) for sustainable mining management. *J Environ Inform* 35(2)
- Ataie-Ashtiani B, Rajabi MM, Ketabchi H (2013). Inverse modelling for freshwater lens in small islands: Kish Island, Persian Gulf. *Hydrological Processes* 27(19): 2759-2773.
- Atlas RM (1975) Effects of temperature and crude oil composition on petroleum biodegradation. *Applied microbiology* 30(3): 396-403.
- Atlas RM (1981) Microbial degradation of petroleum hydrocarbons: an environmental perspective. *Microbiological reviews* 45(1): 180.
- Atlas RM (1985) Effects of hydrocarbons on microorganisms and petroleum biodegradation in arctic ecosystems. *Petroleum effects in the arctic environment* 63-100.
- Atlas RM (1995) Petroleum biodegradation and oil spill bioremediation. *Marine pollution bulletin* 31(4-12): 178-182.
- Atlas RM, Hazen TC (2011) Oil biodegradation and bioremediation: a tale of the two worst spills in US history. In: ACS Publications.
- Bailey J, Ollis D (1986) P 78. *Biochemical engineering fundamentals. 2nd edition. McGraw-Hill, New York.*
- Bakhtyar R, Brovelli A, Barry DA, Robinson C, Li L (2013) Transport of variable-density solute plumes in beach aquifers in response to oceanic forcing. *Advances in Water Resources* 53: 208-224.
- Baldwin AH, Egnotovitch MS, Clarke E (2001) Hydrologic change and vegetation of tidal freshwater marshes: field, greenhouse, and seed-bank experiments. *Wetlands* 21(4): 519-531.
- Bartha R, Bossert I (1984) The treatment and disposal of petroleum wastes.
- Bhosale D, Kumar C (2002) Simulation of seawater intrusion in Ernakulam coast, Proceeding of International Conference on Hydrology and Watershed Management, Hyderabad, 390–399
- Bi H, An C, Chen X, Owens E, Lee K (2020) Investigation into the oil removal from sand using a surface washing agent under different environmental conditions. *J Environ Manage* 275: 111232
- Boll M, Heider J (2010) Anaerobic degradation of hydrocarbons: mechanisms of C–H-bond activation in the absence of oxygen. In *Handbook of Hydrocarbon and Lipid Microbiology*.
- Borden RC, Bedient PB (1986) Transport of dissolved hydrocarbons influenced by oxygen-limited biodegradation: 1. Theoretical development. *Water Resources Research* 22(13): 1973-1982.
- Boufadel MC (2000) A mechanistic study of nonlinear solute transport in a groundwater–surface water system under steady state and transient hydraulic conditions. *Water Resources Research* 36(9): 2549-2565.

- Boufadel MC, Abdollahi-Nasab A, Geng X, Galt J, Torlapati J (2014) Simulation of the landfall of the Deepwater Horizon oil on the shorelines of the Gulf of Mexico. *Environmental science & technology* 48(16): 9496-9505.
- Boufadel MC, Geng X, Short J (2016) Bioremediation of the Exxon Valdez oil in Prince William sound beaches. *Marine pollution bulletin* 113(1-2): 156-164.
- Boufadel MC, Sharifi Y, Van Aken B, Wrenn BA, Lee K (2010) Nutrient and oxygen concentrations within the sediments of an Alaskan beach polluted with the Exxon Valdez oil spill. *Environmental science & technology* 44(19): 7418-7424.
- Boufadel MC, Suidan MT, Venosa AD (1999) A numerical model for density-and-viscosity-dependent flows in two-dimensional variably saturated porous media. *Journal of Contaminant Hydrology* 37(1-2): 1-20.
- Brock TD, Madigan MT, Martinko JM, Parker J (2003) *Brock biology of microorganisms*: Upper Saddle River (NJ): Prentice-Hall 2003.
- Brovelli A, Mao X, Barry D (2007) Numerical modeling of tidal influence on density-dependent contaminant transport. *Water Resources Research* 43(10).
- Brun A, Engesgaard P (2002) Modelling of transport and biogeochemical processes in pollution plumes: literature review and model development. *Journal of Hydrology* 256(3-4): 211-227.
- Caldwell ME, Garrett RM, Prince RC, Suflita JM (1998) Anaerobic biodegradation of long-chain n-alkanes under sulfate-reducing conditions. *Environmental science & technology* 32(14): 2191-2195.
- Chen YM, Abriola LM, Alvarez PJ, Anid PJ, Vogel TM (1992) Modeling transport and biodegradation of benzene and toluene in sandy aquifer material: Comparisons with experimental measurements. *Water Resources Research* 28(7): 1833-1847.
- Cirpka OA, Frind EO, Helmig R (1999) Numerical simulation of biodegradation controlled by transverse mixing. *Journal of Contaminant Hydrology* 40(2): 159-182.
- Clement TP (1999) *A modular computer code for simulating reactive multi-species transport in 3-dimensional groundwater systems*.
- Colombani N, Mastrocicco M, Prommer H, Sbarbati C, Petitta M (2015) Fate of arsenic, phosphate and ammonium plumes in a coastal aquifer affected by saltwater intrusion. *Journal of Contaminant Hydrology* 179: 116-131.
- Colwell RR, Walker JD, Cooney JJ (1977) Ecological aspects of microbial degradation of petroleum in the marine environment. *CRC critical reviews in microbiology* 5(4): 423-445.
- Corapcioglu MY, Baehr AL (1987) A compositional multiphase model for groundwater contamination by petroleum products: 1. Theoretical considerations. *Water Resources Research* 23(1): 191-200.
- Das N, Chandran P (2011) Microbial degradation of petroleum hydrocarbon contaminants: an overview. *Biotechnology research international* 2011.
- Desai AM, Autenrieth RL, Dimitriou-Christidis P, McDonald TJ (2008) Biodegradation kinetics of select polycyclic aromatic hydrocarbon (PAH) mixtures by *Sphingomonas paucimobilis* EPA505. *Biodegradation* 19(2): 223-233.
- Dojka MA, Hugenholtz P, Haack S, Pace NR (1998) Microbial diversity in a hydrocarbon-and chlorinated-solvent-contaminated aquifer undergoing intrinsic bioremediation. *Applied and Environmental Microbiology* 64(10): 3869-3877.
- El-Bihery MA (2009) Groundwater flow modeling of quaternary aquifer Ras Sudr, Egypt. *Environmental geology* 58(5): 1095-1105.

- El-Kadi AI (2001) Modeling hydrocarbon biodegradation in tidal aquifers with water-saturation and heat inhibition effects. *Journal of Contaminant Hydrology* 51(1-2): 97-125.
- Essaid HI (1994) *Simulation of flow and transport processes at the Bemidji, Minnesota, crude-oil spill site*. Paper presented at the Symposium on Natural Attenuation of Ground Water.
- Essaid HI, Bekins BA, Cozzarelli IM (2015) Organic contaminant transport and fate in the subsurface: Evolution of knowledge and understanding. *Water Resources Research* 51(7): 4861-4902.
- Essaid HI, Bekins BA, Godsy EM, Warren E, Baedecker MJ, Cozzarelli IM (1995) Simulation of aerobic and anaerobic biodegradation processes at a crude oil spill site. *Water Resources Research* 31(12): 3309-3327.
- Essaid HI, Cozzarelli IM, Eganhouse RP, Herkelrath WN, Bekins BA, Delin GN (2003) Inverse modeling of BTEX dissolution and biodegradation at the Bemidji, MN crude-oil spill site. *Journal of Contaminant Hydrology* 67(1-4): 269-299.
- Fingas M, Brown CE (2011) Oil spill remote sensing: a review. In *Oil spill science and technology* (pp. 111-169): Elsevier.
- Gao H, Zhang S, Zhao R, Xu D, Zhu L (2018) *Numerical simulation and prediction of groundwater environmental contamination in a coastal polyurethane plant based on GMS*. Paper presented at the MATEC Web of Conferences.
- Geng X, Boufadel MC (2015) Numerical study of solute transport in shallow beach aquifers subjected to waves and tides. *Journal of Geophysical Research: Oceans* 120(2): 1409-1428.
- Geng X, Boufadel MC, Cui F (2017) Numerical modeling of subsurface release and fate of benzene and toluene in coastal aquifers subjected to tides. *Journal of Hydrology* 551: 793-803.
- Geng X, Boufadel MC, Lee K, Abrams S, Suidan M (2015) Biodegradation of subsurface oil in a tidally influenced sand beach: Impact of hydraulics and interaction with pore water chemistry. *Water Resources Research* 51(5): 3193-3218.
- Geng X, Boufadel MC, Personna YR, Lee K, Tsao D, Demicco ED (2014) BioB: a mathematical model for the biodegradation of low solubility hydrocarbons. *Marine pollution bulletin* 83(1): 138-147.
- Geng X, Boufadel MC, Rajaram H, Cui F, Lee K, An C (2020) Numerical study of solute transport in heterogeneous beach aquifers subjected to tides. *Water Resources Research* 56(3): e2019WR026430.
- Geng X, Heiss JW, Michael HA, Boufadel MC (2017) Subsurface flow and moisture dynamics in response to swash motions: Effects of beach hydraulic conductivity and capillarity. *Water Resources Research* 53(12): 10317-10335.
- Geng X, Michael HA, Boufadel MC, Molz FJ, Gerges F, Lee K (2020) Heterogeneity affects intertidal flow topology in coastal beach aquifers. *Geophysical Research Letters* 47(17): e2020GL089612.
- Ghazal KA, Leta O, El-Kadi AI, Dulai H (2018) Quantifying Dissolved Silicate Fluxes across Heeia Shoreline in Hawaii via Integrated Hydrological Modeling Approach. *Univers. J. Geosci* 6: 147-156.
- Godsy EM, Warren E, Cozzarelli IM, Bekins BA, Eganhouse RP (1999) *Determining BTEX Biodegradation Rates Using In Situ Microcosms at the Bemidji site*. Paper presented at the US Geological Survey Toxic Substances Hydrology Program: Proceedings of the Technical Meeting, Charleston, South Carolina, March 8-12: 1999.

- Golchin I, Moghaddam MA (2013) Numerical investigation of contaminant transport in Iranshahr plain aquifer, Iran. *Fresenius Environmental Bulletin* 22(1): 128-135.
- Hamed MM (2005) Screening level modeling of long-term impact of petroleum hydrocarbon contamination on fresh groundwater lenses in the Arabian Gulf region. *Environmental Modeling & Assessment* 9(4): 253-264.
- Haritash A, Kaushik C (2009) Biodegradation aspects of polycyclic aromatic hydrocarbons (PAHs): a review. *Journal of hazardous materials* 169(1-3): 1-15.
- He L, Li Y, Zhu F, Sun X, Herrmann H, Schaefer T, Zhang Q, Wang S (2020) Insight into the mechanism of the OH-induced reaction of ketoprofen: A combined DFT simulation and experimental study. *J Environ Inform* 35(2)
- Heiss J (2011) *Intertidal mixing zone dynamics and swash induced infiltration in a sandy beach aquifer, Cape Henlopen, Delaware*. University of Delaware,
- Heiss JW, Michael HA (2014) Saltwater-freshwater mixing dynamics in a sandy beach aquifer over tidal, spring-neap, and seasonal cycles. *Water Resources Research* 50(8): 6747-6766.
- Jakobsen R, Postma D (1999) Redox zoning, rates of sulfate reduction and interactions with Fe-reduction and methanogenesis in a shallow sandy aquifer, Rømø, Denmark. *Geochimica et Cosmochimica Acta* 63(1): 137-151.
- Jorgensen S, Gromiec MJ (1989) Mathematical submodels in water quality systems.
- Khaska M, La Salle CLG, Lancelot J, Mohamad A, Verdoux P, Noret A, Simler R (2013) Origin of groundwater salinity (current seawater vs. saline deep water) in a coastal karst aquifer based on Sr and Cl isotopes. Case study of the La Clape massif (southern France). *Applied geochemistry* 37: 212-227.
- Kheirandish M, Rahimi H, Kamaliardakani M, Salim R (2020) Obtaining the effect of sewage network on groundwater quality using MT3DMS code: Case study on Bojnourd plain. *Groundwater for Sustainable Development* 11: 100439.
- Lathashri U, Mahesha A (2016) Predictive simulation of seawater intrusion in a tropical coastal aquifer. *J Environ Eng* 142(12): D4015001
- Leahy JG, Colwell RR (1990) Microbial degradation of hydrocarbons in the environment. *Microbiology and Molecular Biology Reviews* 54(3): 305-315.
- Leahy JG, Colwell RR (1990) Microbial degradation of hydrocarbons in the environment. *Microbiol Mol Biol Rev* 54(3): 305-315
- Lee K, Boufadel MC, Chen B, Foght J, Hodson P, Swanson S, Venosa A (2015) Expert panel report on the behaviour and environmental impacts of crude oil released into aqueous environments. *Royal Society of Canada, Ottawa, ON*
- Lee SY, Choi J (1999) Production and degradation of polyhydroxyalkanoates in waste environment. *Waste Management* 19(2): 133-139.
- Li B (2015) *Influence of Petroleum Deposit Geometry on Long Term Persistence of Residual Crude Oil*. Virginia Tech,
- Li H, Boufadel MC (2010). Long-term persistence of oil from the Exxon Valdez spill in two-layer beaches. *Nature Geoscience* 3(2): 96-99.
- Li H, Boufadel MC, Weaver JW (2008) Tide-induced seawater-groundwater circulation in shallow beach aquifers. *Journal of Hydrology* 352(1-2): 211-224.
- Liu Y, Jiao JJ, Luo X (2016) Effects of inland water level oscillation on groundwater dynamics and land-sourced solute transport in a coastal aquifer. *Coastal Engineering* 114: 347-360.

- Liu Z, Liu J, Zhu Q, Wu W (2012) The weathering of oil after the Deepwater Horizon oil spill: insights from the chemical composition of the oil from the sea surface, salt marshes and sediments. *Environmental research letters* 7(3): 035302.
- Lu G, Clement TP, Zheng C, Wiedemeier TH (1999) Natural attenuation of BTEX compounds: model development and field-scale application. *Ground Water* 37(5): 707-717.
- Lyngkilde J, Christensen TH (1992) Redox zones of a landfill leachate pollution plume (Vejen, Denmark). *Journal of Contaminant Hydrology* 10(4): 273-289.
- Mehl SW, Hill MC (2001) User guide to the Link-AMG (LMG) package for solving matrix equations using an algebraic multigrid solver. U.S. Geological Survey Open File Report 01-177. Reston. *USGS, Virginia*
- Medina-Bellver JI, Marín P, Delgado A, Rodríguez-Sánchez A, Reyes E, Ramos JL, Marqués S (2005) Evidence for in situ crude oil biodegradation after the Prestige oil spill. *Environmental microbiology* 7(6): 773-779.
- Mehl SW, Hill MC (2001) *MODFLOW-2000, the US Geological Survey Modular Ground-water Model: User Guide to the Link-AMG (LMG) Package for Solving Matrix Equations Using an Algebraic Multigrid Solver* (Vol. 1): US Department of the Interior, US Geological Survey.
- Mitsch WJ, Gosselink JG, Zhang L, Anderson CJ (2009). *Wetland ecosystems*: John Wiley & Sons.
- Nicol JP, Wise WR, Molz FJ, Benefield LD (1994) Modeling biodegradation of residual petroleum in a saturated porous column. *Water Resources Research* 30(12): 3313-3325.
- Owens E, Sergy G, McGuire B, Humphrey B (1993) *The 1970 Arrow oil spill: What remains on the shoreline 22 years later?* Retrieved from
- Perry J (1984) Microbial metabolism of cyclic alkanes. *Petroleum microbiology* 61-98.
- Porter D, Mayer P, Fingas M (2004) Analysis of petroleum resins using electrospray ionization tandem mass spectrometry. *Energy & fuels* 18(4): 987-994.
- Prince RC (1993) Petroleum spill bioremediation in marine environments. *Critical reviews in microbiology* 19(4): 217-240.
- Ramakrishnan A, Blaney L, Kao J, Tyagi RD, Zhang TC, Surampalli RY (2015) Emerging contaminants in landfill leachate and their sustainable management. *Environmental Earth Sciences* 73(3): 1357-1368.
- Reardon KF, Mosteller DC, Bull Rogers JD (2000) Biodegradation kinetics of benzene, toluene, and phenol as single and mixed substrates for *Pseudomonas putida* F1. *Biotechnology and bioengineering* 69(4): 385-400.
- Reddy CM, Arey JS, Seewald JS, Sylva SP, Lemkau KL, Nelson RK, Ventura GT (2012) Composition and fate of gas and oil released to the water column during the Deepwater Horizon oil spill. *Proceedings of the National Academy of Sciences* 109(50): 20229-20234.
- Robinson C, Brovelli A, Barry D, Li L (2009) Tidal influence on BTEX biodegradation in sandy coastal aquifers. *Advances in Water Resources* 32(1): 16-28.
- Robinson C, Gibbes B, Carey H, Li L (2007) Salt-freshwater dynamics in a subterranean estuary over a spring-neap tidal cycle. *Journal of Geophysical Research: Oceans* 112(C9).
- Rodgers RP, Marshall AG (2007) Petroleomics: Advanced characterization of petroleum-derived materials by Fourier transform ion cyclotron resonance mass spectrometry (FT-ICR MS). In *Asphaltenes, heavy oils, and petroleomics* (pp. 63-93): Springer.
- Rojo F (2009) Degradation of alkanes by bacteria. *Environmental microbiology* 11(10): 2477-2490.

- Santos F, DeCastro M, Gómez-Gesteira M, Álvarez I (2012) Differences in coastal and oceanic SST warming rates along the Canary upwelling ecosystem from 1982 to 2010. *Continental Shelf Research* 47: 1-6.
- Sbarbati C, Colombani N, Mastrocicco M, Aravena R, Petitta M (2015) Performance of different assessment methods to evaluate contaminant sources and fate in a coastal aquifer. *Environmental Science and Pollution Research* 22(20): 15536-15548.
- Schäfer W, Therrien R (1995) Simulating transport and removal of xylene during remediation of a sandy aquifer. *Journal of Contaminant Hydrology* 19(3): 205-236.
- Schulze-Makuch D (2005) Longitudinal dispersivity data and implications for scaling behavior. *Groundwater* 43(3): 443-456
- Shrestha N, Wang J (2020) Water quality management of a cold climate region watershed in changing climate. *J Environ Inform* 35(1)
- Speight JG (2007) *Hydroprocessing of heavy oils and residua*: CRC Press.
- Steeffel C, Appelo C, Arora B, Jacques D, Kalbacher T, Kolditz O, . . . Meeussen J (2015) Reactive transport codes for subsurface environmental simulation. *Computational Geosciences* 19(3): 445-478.
- Suk H (2017) Semi-analytical solution of land-derived solute transport under tidal fluctuation in a confined aquifer. *Journal of Hydrology* 554: 517-531.
- Torlapati J, Boufadel MC (2014) Evaluation of the biodegradation of Alaska North Slope oil in microcosms using the biodegradation model BIOB. *Frontiers in microbiology* 5: 212.
- Ulrici W (2000) Contaminated soil areas, different countries and contaminants, monitoring of contaminants. *Biotechnology: Environmental Processes II* 11: 5-41.
- Uraizee FA, Venosa AD, Suidan MT (1997) A model for diffusion controlled bioavailability of crude oil components. *Biodegradation* 8(5): 287-296.
- Venosa AD, Campo P, Suidan MT (2010) Biodegradability of lingering crude oil 19 years after the Exxon Valdez oil spill. *Environmental science & technology* 44(19): 7613-7621.
- Venosa AD, Suidan MT, Wrenn BA, Strohmeier KL, Haines JR, Eberhart BL, . . . Holder E (1996) Bioremediation of an experimental oil spill on the shoreline of Delaware Bay. *Environmental science & technology* 30(5): 1764-1775.
- Verma DK, Tombe Kd (2002) Benzene in gasoline and crude oil: occupational and environmental implications. *AIHA Journal* 63(2): 225-230.
- Vilcáez J, Li L, Hubbard SS (2013) A new model for the biodegradation kinetics of oil droplets: application to the Deepwater Horizon oil spill in the Gulf of Mexico. *Geochemical transactions* 14(1): 4.
- Vroblecky DA, Chapelle FH (1994) Temporal and spatial changes of terminal electron-accepting processes in a petroleum hydrocarbon-contaminated aquifer and the significance for contaminant biodegradation. *Water Resources Research* 30(5): 1561-1570.
- Waddill D, Widdowson M (2002) SEAM3D-A numerical model for three-dimensional solute transport coupled to sequential electron acceptorbased biological reactions in groundwater. Vicksburg, MS. *US Army Corps of Engineers*.
- Waddill DW, Widdowson MA (1998) Three-dimensional model for subsurface transport and biodegradation. *Journal of Environmental Engineering* 124(4): 336-344.
- Walker J (1984) chemical fate of toxic-substances-biodegradation of petroleum. in (vol. 18, pp. 73-86): marine technology soc inc c/o clayton matthews, 1828 1 st, nw, 9th fl
- Wang Z, Fingas M, Page DS (1999) Oil spill identification. *Journal of Chromatography A*, 843(1-2): 369-411.

- Widdowson MA, Molz FJ, Benefield LD (1988) A numerical transport model for oxygen-and nitrate-based respiration linked to substrate and nutrient availability in porous media. *Water Resources Research* 24(9): 1553-1565.
- Xia WX, Li JC, Zheng XL, Bi X, Shao J (2006) Enhanced biodegradation of diesel oil in seawater supplemented with nutrients. *Engineering in Life Sciences* 6(1): 80-85.
- Xia Wx, Zheng Xl, Li Jc, Song Zw, Zhou L, Sun Hf (2005) Degradation of crude oil by indigenous microorganisms supplemented with nutrients. *Journal of Environmental Sciences* 17(4): 659-661.
- Xin P, Robinson C, Li L, Barry DA, Bakhtyar R (2010) Effects of wave forcing on a subterranean estuary. *Water Resources Research* 46(12).
- Xu Z, Chai J, Wu Y, Qin R (2015) Transport and biodegradation modeling of gasoline spills in soil-aquifer system. *Environmental Earth Sciences* 74(4): 2871-2882.
- Young L, Gibson D (1984) Microbial degradation of organic compounds. In: Marcel Dekker New York.
- Zhai A, Ding X, Zhao Y, Xiao W, Lu B (2020) Improvement of instantaneous point source model for simulating radionuclide diffusion in oceans under nuclear power plant accidents. *Journal of Environmental Informatics* 36(2): 133-145.